Greenhouse gas emissions (CO2 and CH4) and inorganic carbon behavior in an urban highly polluted tropical coastal lagoon (SE, Brazil)

Luiz Cotovicz, Renato Ribeiro, Carolina Ramos Régis, Marcelo Bernardes, Rodrigo Sobrinho, Luciana Oliveira Vidal, Daniel Tremmel, Bastiaan Knoppers, Gwenaël Abril

Greenhouse gas emissions (CO_2 and CH_4) and inorganic carbon in an urban tropical coastal lagoon (Jacarepagua Lagoon Complex, Brazil)

Luiz C. Cotovicz, Jr.*[a,b]; Renato P. Ribeiro[c]; Carolina Ramos Régis[b]; Marcelo Bernardes[b]; Rodrigo Sobrinho[b]; Luciana Oliveira Vidal[d]; Daniel Tremmel[b]; Bastiaan A. Knoppers[b]; Gwenaël Abril[b,e]

Affiliations

a Instituto de Ciências do Mar, Universidade Federal do Ceara, Fortaleza, CE, Brazil

b Programa de Geoquímica, Universidade Federal Fluminense, Niterói, RJ, Brazil

c Centro Experimental de Monitoramento e Mitigação Ambiental (CEMMA), Instituto Federal de Educação, Ciência e Tecnologia do Rio de Janeiro (IFRJ), Nilópolis, RJ, Brasil

d Laboratório de Ciências Ambientais, Centro de Biociências e Biotecnologia Universidade Estadual do Norte Fluminense, Campos dos Goytacazes, RJ, Brazil

e Biologie des Organismes et Ecosystèmes Aquatiques (BOREA), UMR 7208, Muséum National d'Histoire Naturelle, CNRS, IRD, SU, UCN, UA, Paris, France.

* Corresponding Author: lccjunior@id.uff.br; Telephone Number (+55 21 995645663); ORCID 0000-0002-3914-8155

Published in : Environmental Science and Pollution Research

https://doi.org/10.1007/s11356-021-13362-2

Highlights

- Oxygen-depleted river waters were associated with high concentrations of TA and DIC
- TA and DIC decreased in the mixing region due to re-oxidation processes
- Extreme high concentrations and emissions of CO_2 and CH_4 were found in hypoxic/anoxic polluted river waters
- Concentrations and emissions of GHG decreased seaward direction as results of mixing, degassing and biological uptake
- The diffusive CH_4 emissions were more important than CO_2 emissions in terms of global warming potential

Abstract

Increasing eutrophication of coastal waters have been associated with disturbances in greenhouse gases (GHGs) concentrations and emissions to the atmosphere, but still overlooked globally. Here, we investigated the concentrations and diffusive fluxes of carbon dioxide (CO_2) and methane (CH_4) in the urban-dominated Jacarepagua Lagoon Complex (JLC) (Southeastern Brazil). This lagoonal complex presents high polluted and eutrophic waters, showing frequent occurrences of anoxia and hypoxia, and phytoplankton blooms. Between 2017 and 2018, four spatial surveys were performed (dry and wet conditions) in the system, with sampling in the river waters that drain the urban watershed, and in the lagoon waters. Strong oxygen depletion was found in the polluted rivers, associated with high values of partial pressure of CO2 (pCO_2) and CH_4 concentrations. These rivers receive massive amounts of organic matter and nutrients from untreated domestic effluents. The high GHGs concentrations are attributed to organic matter degradation mediated by aerobic and anaerobic processes, with concomitant production of total alkalinity (TA) and dissolved inorganic carbon (DIC). In the lagoon, GHGs concentrations decreased due to dilution with seawater, degassing and phytoplankton growth. TA concentrations were minimal at salinity of ~20 suggesting processes of organic matter re-oxidation during estuarine mixing. Emissions of CO_2 ranged from 22 to 48 mmol C m^{-2} d^{-1}, and those of CH_4 from 2.2 to 16.5 mmol C m^{-2} d^{-1}, this later among the highest documented in coastal waters. Compared in terms of global warming potential (GWP), the diffusive emissions of CH_4 were more important than CO_2 emissions. These results highlight that high-polluted coastal ecosystems are hotspots of GHGs emissions to the atmosphere, and must be included in global budgetary assertions.

Key-words: Greenhouse Gas Emissions, Carbon Dioxide, Methane, Carbonate Chemistry, Coastal Eutrophication, Coastal Lagoons

1.Introduction

Coastal eutrophication is one of the major environmental threats to coastal ecosystems worldwide, and particularly accelerated and severe in ecosystems densely populated (Nixon 1995; Cloern 2001, Bricker et al. 2008). At advanced stages of eutrophication, the high nutrient and organic matter enrichment lead to profound changes in ecosystem metabolism and biogeochemical cycling, deteriorating the ecological health and water quality. Some

adverse effects include occurrence of harmful algal blooms (HABs), accelerate growth of fungal and bacterial communities, oxygen depletion, and coastal acidification (Bricker et al. 2008; Cai et al. 2011). Studies have suggested that coastal eutrophication has been perturbing the carbon cycling, leading to alteration in carbon budgets and greenhouse gas emissions (GHGs), such as carbon dioxide (CO_2) and methane (CH_4) (Howarth et al. 2011). CO_2 and CH_4 are the principal well-mixed and long-lived GHGs present in the atmosphere and, together, these gases answer to more than 80% of the actual increase in the global average atmospheric temperature (IPCC 2013). Global mean atmospheric CO_2 concentrations increase from 280 ppmv during the pre-Industrial Revolution (Siegenthaler et al. 2005), to reach actual concentration overpassing 415 ppmv (NOAA 2019). For CH_4, a more powerful GHG, the concentration changed from 0.72 ppmv in the pre-Industrial period (Etheridge et al. 1998) to the current level of about 1.80 ppmv (NOAA 2019). Despite of this well-documented atmospheric rise, the sources and sinks of these GHGs in the diverse compartments of the Earth global system are not yet properly understood and quantified, particularly in disturbed coastal ecosystems at subtropical and tropical latitudes.

The low levels of oxygen concentrations in coastal waters are associated with high levels of aquatic partial pressure of CO2 (pCO_2), enhancing the CO_2 degassing and coastal acidification (Cai et al. 2011). In this way, coastal eutrophication can act amplifying the CO_2 emissions by stimulating heterotrophic processes through the respiration of anthropogenic-derived organic carbon (Frankignoulle et al. 1998; Zhai et al. 2007). The internal processes of respiration of organic matter in eutrophic aquatic ecosystems modifies not only the CO_2 concentrations, but all the parameters of the carbonate chemistry, with influences on the acid-base properties, altering the pH, and concentrations of total alkalinity (TA) and dissolved inorganic carbon (DIC) (Abril and Frankignoulle 2001; Cai et al. 2011; Sunda and Cai 2012; Cotovicz et al. 2018). However, eutrophication can also contributes to promote CO_2 sink by stimulating the primary production with important CO_2 uptake in coastal waters that receives important amounts of nutrients (Borges and Gypens 2010; Cotovicz et al. 2015, 2020; Kubo et al. 2017). In this regard, eutrophication can both amplify CO_2 outgassing (when organic matter is intensely degraded by microbial activities) or CO_2 ingassing (when organic matter is intensely produced by primary producers). These interplays between sources and sinks of CO_2 and alteration in carbonate chemistry depends on local/regional characteristics, and are not well-understood.

For CH_4, the eutrophication is related to increasing concentrations in aquatic compartments. Pristine rivers are usually organic matter poor-environments and weak sources of CH_4 compared to impacted ecosystems (Richey et al. 1988; Purvaja and Ramesh 2000; Brigham et al. 2019). The production of CH_4 increases with hypoxic and anoxic conditions associated to the increased inputs of organic matter to water and sediments. In coastal waters, the CH_4 production is most important in low salinity regions, where methanogenesis is promoted by the low availability of electron acceptors (Chanton et al. 1989; Kelley et al. 1990); in high salinity regions sulphate reduction outcompetes with methanogenesis as the main pathway of sedimentary anaerobic organic matter degradation (Martens and Klump 1980; Martens et al. 1998). In coastal marine sediments with high salinity, large inputs of organic matter are necessary for methanogenesis to occur and generate CH_4 rich gassy-sediments (Martens and Klump 1980; Martens et al. 1998). It is particularly relevant the contributions from wastewater treatment plants and direct inputs from untreated domestic effluents that are rich in CO_2 and CH_4 in disturbed coastal ecosystems (Nirmal-Rajkumar et al. 2008; Burgos et al. 2015; Cotovicz et al. 2016; Brigham et al. 2019). This means that regions under influence and/or close to sewage discharge present higher CO_2 and CH_4 concentrations and emissions. In addition, it is important to point that anaerobic respiration processes (such as denitrification, manganese reduction, iron reduction and sulfate reduction), produce TA, and in some cases also involve alteration in DIC concentrations (Abril and Frankignoulle 2001; Rassmann et al. 2020).

Coastal lagoons represent an estuarine typology highly sensitive to develop eutrophication due to the long residence times and due to host large human settlements (Knoppers et al. 1999). These near-shore coastal environments occurs in 13% of the World's coastline (Kjerfve 1985), normally exhibiting high levels of primary production (Knoppers et al. 1999). There have been very few studies conducted in coastal lagoons regarding the assessment of concentrations and quantification of emissions of GHGs, particularly in tropical regions (Borges and Abril 2011, Koné et al. 2009, 2010), creating large uncurtains in global GHG budgets. In the present study, we analyze and quantify the concentrations and fluxes of CO_2 and CH_4 in a high-polluted and urban-dominated coastal lagoon, the Jacarepagua Lagoon Complex (JLC), located at the Rio de Janeiro coast (Southeastern, Brazil). The system hosts a population near of 1 million of inhabitants along the watershed (Santos Neves et al. 2017). We hypothesized that the strong pollution and eutrophication will contribute with high emissions of GHG in this system, especially in the riverine waters that receive high loads of organic matter and nutrients from untreated urban effluents (Fig. 1). For this, we constructed a sampling design turned to contrast riverine and lagoonal

conditions, by choosing 05 stations in river waters, and 05 stations in lagoon waters. Our results showed extremely high concentrations and emissions of CO_2 and CH_4 in anoxic/hypoxic freshwaters. The concentrations and emissions of CO_2 and CH_4 in the freshwaters are among the highest documented in coastal waters worldwide, and are hotspots of GHGs emissions.

2.Material and Methods

2.1.Study Area

The JLC (Lat. 22°55'S and 23°03'S; Long. 43°30'O and 43°18'O) is located in the west region of the Rio de Janeiro City (Southeastern Brazil). The system is composed by four coastal lagoons: Jacarepaguá (Area = 4.07 km^2), Camorim (A = 0.80 km^2), Tijuca (A=4.34 km^2) and Marapendi (A = 3.33 km^2) (Fig. 1). The total surface area covers about 12.8 km^2, and the drainage basin extends over approximately 280 km^2 (Salloto et al. 2012). The water volume in the lagoon is estimated at about 2.38 $x10^7$ m^3 (Sampaio 2008). The annual freshwater inputs to the system are weak, about 3.00 m^3 s^{-1} (Sampaio 2008). However, under strong levels of precipitation, the freshwater inflow can be significantly higher. These lagoons present microtidal amplitude, are enclosured and connected to the sea by only one channel, the Joa Channel (Gomes et al. 2009). The climate in the region is classified as tropical humid, with a wet warm summer and a dry winter (Sampaio 2008). This lagoon complex has been suffering with intense anthropogenic activities developed in its surroundings and along the watershed, mainly urbanization and industrialization (Gomes et al. 2009). Actually, the human population surrounding the JLC is about 1 million of inhabitants, reflecting in high loads of domestic and industrial effluents discharged directly into the water body and its rivers. The wastewater services collection are still very precarious and inefficient, covering only about 60% of the total produced (ANA 2019). Taking account the population of the watershed and the estimates of emissions of effluents per capita (Wallace 2005), the amount of effluents discharges are on the same order of the freshwater inputs to the system (~ 3.4 m^3 s^{-1}), i.e., the mean wastewater volume loaded to the lagoon is almost equivalent to the freshwater river loads. This results in a heavily eutrophication process in this system, with perennial presence of cyanobacterial blooms and frequent episodes of hypoxia/anoxia (Gomes et al. 2009; De-Magalhães et al. 2017).

2.2.Sampling Strategy

Four sampling campaigns were conducted in the months of March-2017, June-2017, November-2017 and May-2018. In each sampling campaign, five stations were sampled on the rivers that compose the drainage basin of the lagoon complex, and five stations were sampled in the lagoons of Tijuca and Marapendi (Fig. 1). The sampling stations in the rivers were accessed by car. The sampling stations in the lagoons were accessed using a small boat. The depths of the sampling stations were always lower than 2.5 m. A Niskin bottle model Alfakit 3L was used to collect water samples in sub-surface (~0.5 m depth). The samples were conditioned (fixed and or/ maintained in ice in the dark) for further analysis in the laboratory. A calibrated multiparametric Sonde (YSI Professional Plus) measured *in situ* the salinity, temperature, and levels of dissolved oxygen (DO). The samplings were always conducted during the ebb tide, to assess the major contribution from land runoff. Important to point that we were not allowed to access the lagoons of Camorim and Jacarepagua due to the presence of an "ecological barrier", which prevented the boat navigation inside these water bodies (Fig. 1).

2.3.Laboratory analysis

Whatman GF/F filtres were used for chlorophyll *a* (Chl *a*) analysis, and the filtrate for nutrients and total alkalinity (TA) analysis. All the filters were pre-combusted (at 500° C for 6 h). Chl *a* concentrations were extracted in 90% acetone and quantified spectrophotometrically before and after acidification of the samples, with formulations and corrections proposed by Lorenzen (1967). Dissolved inorganic nitrogen, including ammonium (NH_4^+), nitrite (NO_2^-), and nitrate (NO_3^-) were quantified by the colorimetric method as in Grasshoff et al. (1999). TA was determined on 60 mL of filtrate using the Gran (1952) electro-titration method with an automated titration system (Metler Toledo model T50). The reproducibility of TA was about 3 μmol kg^{-1} (n = 7). Measurements were compared to certified reference material (CRM, provided by A. G. Dickson from Scripps Institution of Oceanography) and consistent at a maximum accuracy level of 5 μmol kg^{-1}. pH was measured with a WTW 3310 pH meter equipped with a Sentix 41 electrode, calibrated in the National Institute of Standards and Technology (NIST) scale, using a three point standard (pH 4.01, pH 7.00 and pH 10.01), always before and after each sampling campaign. The precision of the pH measurements was about 0.01 (after seven verifications against standards).

Samples for dissolved CH_4 were collected in 30 ml, of pre-weighted serum glass bottles, completely filled with water using a homemade sampler that prevents gas exchanges and bubble formation. After sealed, 0.2 ml of saturated mercuric chloride were added in all bottles to prevent microbial activities. In the laboratory, a headspace of 10 mL of N_2 were created in the samples, followed by a vigorous agitation to obtain a complete equilibrium between the air and water phases inside the bottles. CH_4 concentrations were determined by gas chromatography (GC) with flame ionization (FI methanizer detector) (Abril et al. 2007). In situ CH_4 concentrations were calculated taking account the volume of water and headspace in the vial and solubility coefficient of methane of Yamamoto et al. (1976), as function of temperature and salinity. Reproducibility of the CH_4 analysis was better than 5%.

2.4.Calculations

2.4.1.Carbonate System

The pCO_2 values and DIC concentrations were calculated using the concentrations of TA, pH, nutrients, seawater temperature, and salinity by the CO2calc 1.2.9 program (Robbins et al. 2010). The dissociation constants for carbonic acid were those proposed by Mehrbach et al. (1973) refitted by Dickson and Millero (1987), the borate acidity constant from Lee et al. (2010), the dissociation constant for the HSO_4^- ion from Dickson (1990) and the CO_2 solubility coefficient of Weiss (1974). For the anoxic/hypoxic waters we calculated the pCO_2 and DIC using the update version of the program CO2SYS that include acid-base system of NH_4^+ to TA (Xu et al. 2017).

2.4.2.The excess of DIC (E-DIC) and Apparent Utilization of Oxygen (AOU)

The excess of DIC (E-DIC, μmol kg^{-1}) was calculated according to Abril et al. (2003):

$$E\text{-}DIC = DIC_{sample} - DIC_{equilibrium},$$

Where DIC_{sample} represents the measured concentration of DIC (μmol kg^{-1}) and $DIC_{equilibrium}$ is the theoretical DIC at atmospheric equilibrium (μmol kg^{-1}). $DIC_{equilibrium}$ was calculated from observed TA and the atmospheric pCO_2 measured in the estuary.

The apparent oxygen utilization (AOU, μmol kg^{-1}) was calculated as proposed by Benson and Krause (1984):

$$AOU = DO_{equilibrium} - DO_{sample}$$

Where DO_{sample} is the measured DO, and $DO_{equilibrium}$ is the DO saturation.

2.4.3.End-Member Mixing Models

We applied mixing models to investigate the gains and losses of TA, DIC and δ^{13}C-DIC along the estuary. The model assumes conservative mixing for a solute (E) according to (Samanta et al. 2015):

$$E_{mix} = E_{freshwater}F_{freshwater} + E_{marine}(1 - F_{freshwater})$$

Where E_{mix} is the concentration of a given solute during conservative mixing (in our case TA and DIC), and the subscripts freshwater and marine indicate the endmember concentrations in the river and the ocean, respectively. The freshwater fraction ($F_{freshwater}$) is calculated as:

$$F_{freshwater} = 1 - Sal_{sample}/Sal_{marine}$$

Where Sal is the salinity, the subscript sample refers to the *in situ* values for each station.

2.4.4.Calculations of air-water GHG fluxes

Diffusive fluxes of CO_2 and CH_4 at the air-water interface were computed according to the following equation:

$$F(GHG) = kg,T\ \Delta GHG$$

Where F(GHG) represents the diffusive fluxes of CO_2 and CH_4, kg,T represents the gas transfer velocity of a given gas (g) at a given temperature (T), and the ΔGHG represents the concentration gradient between the water and the water at equilibrium with the overlying atmosphere. The considered atmospheric partial pressure of CO_2 and CH_4 were considered, respectively, 410 ppmv and 1.80 ppmv, which corresponds to global averages of atmospheric GHG concentrations. These values are consistent with previous direct measurements of CO_2 and CH_4 atmospheric concentrations realized near to the study area (Cotovicz et al. 2015, 2016).

For calculate the gas transfer velocity, we first normalized by a Schmidt number, applying the following equation (Jähne et al. 1987):

$$Kg,T = k_{600} (600/Sc_{g,T})^{n}$$

Where k_{600} is the gas transfer velocity normalized to a Schmidt number of 600 (Sc = 600, for CO_2 at a temperature of 20°C), $Sc_{g,T}$ is the Schmidt number of a gas at a giver temperature (Wanninkhof, 1992), and n is related to wind velocity, being equal to 2/3 for wind speed < 3.7 m s^{-1}, and equal to 1/2 for higher wind velocities (Jähne et al. 1987; Guérin et al. 2007).

We used three empirical equations to derive k600 values: the parameterization as a function of wind speed applied for oceanic waters by Wanninkhof (1992, W92), the parameterization as a function of wind speed estimated for estuarine ecosystems by Raymond and Cole (2001, RC01), and the parameterization as a function of wind speed produced by regressing the literature data in coastal environments by Jiang et al. (2008; J08). The three parameterizations cover an important variability of values, with the value of W92 providing the lowest estimations, and that of J08 providing the highest values of k_{600}.

The W92, RC01 and J08 parameterizations can be calculated applying the following equations:

$$k_{600}(W92) = 0.31(U_{10}\text{^}2)$$

$$k_{600}(RC01) = 1.91\exp 0.35U_{10}$$

$$k_{600}(J08) = 0.314(U_{10}\text{^}2) - 0.436U_{10} + 3.99 \text{ (J08)}$$

Where k_{600} is the gas transfer velocity normalized to a Schmidt number of 600 (cm h^{-1}), U_{10} is the wind speed at 10 m height (m s^{-1}), v is the water current velocity in m s^{-1}, and S is the surface area of the estuary in km^2. Water-to-air CO_2 fluxes were calculated using the GHG concentrations for each sampled station. After, these fluxes per station were daily-averaged considering the "polluted rivers" stations (1 to 5) and the "lagoons" stations (5 to 10) using the averaged gas transfer velocities calculated for each day of sampling. Gas transfer velocities were calculated from wind speed data, which were logged every hour and averaged at 12 h intervals throughout the sampling days. The fluxes calculated for each domain, i.e., "polluted rivers" and "lagoons" were separated in nighttime (measurements conducted before 09:30 a.m.) and daytime (measurements conducted after 09:30 a.m.) periods to account for the diel wind patterns and then integrated over the entire sampled period and the entire sampled area. We divided the gas transfer velocities in these periods because the region receive important influences from marine brises, where the winds are stronger during midday/afternoon than during the night/early morning (Amarante et al. 2002; Cotovicz et al. 2015). The meteorological data were kindly provided by the National Institute of Meteorology (INMET). To compare the air-water fluxes of CH_4 with those of CO_2 we used the concepts of global warning potential (GWP) and CO_2 equivalent emissions (CO_2-eq), by considering that 1g of CH_4 has a GWP equivalent to 28g of CO_2 on a time horizon of 100 years (IPCC 2013).

2.5.Statistical Analysis

To verify if the data followed parametric or non-parametric distributions we applied the Shapiro-Wilk test. As the data set was not normally distributed, we used the non-parametric and non-paired Man-Whitney test to compare the average differences between the river and lagoons stations for each sampling camping (spatial variability). The non-parametric and paired Friedman Test was applied to compare the averages of sampled stations considering the different sampling campaigns (temporal variability). Linear and non-linear regressions were calculated to compare the distributions and correlations between variables. All statistical analysis were based on $\alpha = 0.05$. We used the GraphPad Prism 6 program (GraphPad Software, Inc., La Jolla, California) to perform the statistical tests.

3.Results

3.1.Ancillary parameters

The main parameters analyzed in this study are provided in Table 1, with averages, standard deviations, and ranges. The data were separated by sampling campaigns, and by sampled stations (rivers and lagoon). Box plots of the main parameters, separated by sampling stations, with maximum, minimum, and medians are presented in the supplemental file (Online Resource Fig. S1). Water temperature was related to the period of the year. The highest temperatures were measured in summer, reaching a maximum of 29.0°C in Mar-17, whereas the lowest temperatures were measured in winter/autumn, with a minimum of 20.4 °C in Nov-17. The water temperature did

not present significant spatial differences when comparing rivers and lagoon (Mann-Whitney test, $p > 0.05$), except in the campaign of Nov-17, when the lagoon stations presented lower temperature than the freshwaters (Mann-Whitney test, $p < 0.01$). The salinity at river stations was always closest to 0, excepting at stations 4 and 5, which present occasional saline intrusion reaching a maximum value of 5 (Tab. 1, Fig. 2). The salinity in the lagoon stations ranged between 6.6 and 34. As expected, the highest salinities were observed in the stations located closest to the mouth of the lagoon complex (stations 6 and 8).

DO concentrations exhibited strong depletion in the river stations, reaching values very close to 0 in almost all stations and sampling campaigns (Tab. 01; Fig. 2f). Exceptions were verified in the station 4, which exhibited occasional occurrence of high DO concentrations. In the lagoons, the concentrations of DO were variable, usually exhibiting undersaturated conditions, with very little occasions of oversaturation with respect to the atmosphere equilibrium (Fig. 2f). This pattern of DO distributions was inverse of that verified for the concentrations of NH_4^+ (Fig. 2g). The highest values of NH_4^+ were found in the hypoxic/anoxic freshwaters, reaching an extreme maximum concentration of 5,660 μmol L^{-1}. The concentrations of NH_4^+ decreased exponentially with the increase of salinity and with the increase of DO concentrations (Fig. 3a), reaching a minimum of 3.5 μmol L^{-1}. As expected, DO distributions were positively related to the concentrations of NO_3^- (Fig. 3b). NO_3^- exhibited low concentrations in the polluted rivers, with increasing tendency with the increase of salinity and DO concentrations (Fig. 3b). The concentrations of Chl *a* were significantly lower in the freshwaters compared to the lagoon stations (Mann-Whitney test, $p < 0.01$) (Fig. 2h). In general, the anoxic/hypoxic freshwaters presented low concentrations of Chl *a*, excepting at station 4, which presented occasional occurrence of high Chl *a* concentrations, with an extreme highest value of 347 μg L^{-1}, and coincident with a peak in DO concentration (Fig. 2f,h). In the lagoon stations, the distributions of Chl *a* were high variable ("patch distributions"), exhibiting the highest concentrations at intermediate salinities (10-20). The results of Chl *a* for the sampling in May-2018 are not presented due to problems during sampling.

3.2.Carbonate Chemistry

The distributions of TA and DIC were very different considering the river and lagoon stations (Fig. 2a,b). TA and DIC concentrations were significantly higher in freshwaters compared to the lagoon waters (Mann-Whitney test, $p < 0.001$), except in the campaign in Nov-17, when the river TA and DIC concentrations were lower than the lagoons (Fig 2a,b). The ranges of concentrations of freshwater TA were between 572 and 3,680 μmol kg^{-1}, and for DIC these ranges varied between 652 and 4,026 μmol kg^{-1}. Considering the lagoon stations, these ranges varied between 1,431 and 2,567 for TA, and between 1,205 and 2,319 for DIC. DIC and TA distributions did not exhibit a clear pattern with salinity. In the camping in Nov-17, the tendency between TA and DIC versus salinity was positive, whereas for the other three sampling campaigns this relationship was negative. However, in all sampling campaigns the distributions of TA and DIC showed large deviations from the conservative mixing considering the end-member mixing models (Fig. 4). In general, the lagoon stations presented negative values of ΔTA and ΔDIC (Δ representing the differences between measured DIC and/or TA concentrations and the expected value for the conservative mixing), indicating important consumption of DIC and TA in the mixing regions. The highest values of TA were found in hypoxic/anoxic waters, presenting positive relationship with NH_4^+ concentrations and negative relationship with NO_3^- (Fig. 3c,d). A TA minimum was observed in the middle salinity region, corresponding to lowest NH_4^+, highest NO_3^-, DO and Chl *a* concentrations.

As expected, the river waters presented low values of pH, with a minimum value of 6.93, and average of 7.22 ± 0.20 (Tab. 1; Fig. 2d). The pH increased inside the lagoons, presenting the highest concentrations in the intermediate salinities (10-20), and coincident with the highest values of Chl *a*, despite of the absent significant correlation between these parameters. The values of pH were strongly correlated to the distributions of DO concentrations (Fig. 5a).

3.3.Dissolved GHG concentrations and air-water fluxes

As showed for the most parameters analyzed in this study, the averaged values of pCO_2 were highly different considering the "polluted rivers" and "lagoons" for all the sampling campaigns (Tab. 1, Fig. 2c). High supersaturated conditions were observed in the anoxic/hypoxic river waters. The highest pCO_2 value was 20,417 ppmv. Freshwater pCO_2 exceeding 12,000 ppmv were verified in all sampling campaigns. In the lagoons, the values decreased substantially, lowering about one order of magnitude. The average value was 764 ± 320 ppmv in the lagoon stations. Values of pCO_2 below the equilibrium with the atmosphere were verified only in four occasions, being three in the lagoons and one in the river domain, all related to high concentrations of Chl *a* and

oversaturation of DO (Fig. 2c,d,f). Considering all data (river and lagoon stations), the averaged values of pCO_2 were significantly different considering the sampling campaigns ($p < 0.05$; Friedman Test). We used the relationship between the apparent utilization of oxygen (AOU) and the excess of dissolved inorganic carbon (E-DIC) to investigate the influence of biological processes on the concentrations of DIC and DO (Fig. 5b). The scatter plot of E-DIC versus AOU shows that the data of the lagoon stations were close to the 1:1 line. This line represents the theoretical quotient of photosynthesis and respiration. The river stations presented a marked deviation above the 1:1 line, corresponding to hypoxic/anoxic conditions.

For the distributions of CH_4, the behavior was similar to that of pCO_2, exhibiting extreme supersaturation conditions in the hypoxic/anoxic river waters (Figs. 2e, 5c). The highest CH_4 concentration was 288,572 nmol L^{-1}, coincident with anoxic conditions (0.1 $\%O_2$), representing one of the uppermost concentration even reported in coastal waters worldwide. All the concentrations of dissolved CH_4 were higher than 25,000 nmol L^{-1} in the polluted rivers, excepting in one situation in the station 4 (Nov-17), which displayed concentration of 550 nmol L^{-1}, and coincident with the high concentration of Chl *a* and supersaturation of DO. In the lagoons, the CH_4 concentrations decreased exponentially compared to the rivers, spanning between two to three orders of magnitude. CH_4 concentrations in the lagoons ranged between 47 to 4,666 nmol L^{-1}. The CH_4 concentrations were significantly different considering the sampling campaigns, including all data, and the river and lagoons stations separately (rivers x lagoons). The highest concentrations of CH_4 in the river were observed in Nov-2017, which was the sampling with the low rates of accumulated precipitation over 3 days (the precipitation rate reaching the ground over the period of 3 days before sampling). The results of CH_4 in the month of May-2018 are not presented due to logistical problems during sampling.

The relationship between dissolved CH_4 concentrations and pCO_2 values were positive and statistically significant for all sampling campaigns (Fig. 6). However, it is clear that the tendency was different considering the sampled periods, with distinct slopes and intercepts. In two samplings (Mar-2017 and Nov-2017), the relationship showed a linear tendency between these two parameters showing, respectively, the following equations: $Y = 4.21*X - 4179$; $R^2 = 0.97$; $p < 0.0001$ and $Y = 19.81*X - 5119$; $R^2 = 0.91$; $p < 0.0001$. In the sampling of Jun-2017, the relationship followed a non-linear trend, fitting in an exponential growth equation type "one phase decay", with the equation $Y = -6472*69867*\exp(-0.00023*X) + 69867$; $R^2 = 0.81$. This figure also showed that for similar values of pCO_2 (~ 15,000 ppmv), the concentrations of CH_4 can span one order of magnitude (from ~25,500 to 170,000 nmol L^{-1}).

The values of gas transfer velocities as well as fluxes of CH_4 and CO_2 are presented in Table 2. The gas transfer velocities were lower for the calculated with the parametrization of W92, followed by the parameterization of RC01 and J08. The k_{600} values ranged between 0.99 and 5.10 m s^{-1} for the river sampled stations, whereas for the lagoon stations this range was between 1.12 and 6.13 m s^{-1}. In general, the k_{600} did not present significant differences considering the sampling campaigns ($p > 0.05$; Friedman Test), except in the sampling of Nov-17 in the second day of sampling, when the values of wind speed were higher. The calculated diffusive fluxes of CO_2 and CH_4 at the air-water interface showed marked differences considering the river and lagoons stations, with the river showing very higher emissions than the lagoons (Tab. 2). The fluxes calculated for each sampling campaign, including fluxes for the river and lagoon stations separately, as well as the fluxes with all data (area-weighted). The emissions of CO_2 and CH_4, with the averages and standard deviations calculated with the three parameterizations are presented in supplemental file (Online Resource Fig. S2). The river stations always showed high emissions of CO_2, with averages of emissions ranging between 72.85 and 652.48 mmol C $m^{-2}d^{-1}$. For the lagoons, the emissions spanned between one to two orders of magnitude lower than the rivers. The emissions in the lagoons ranged between 4.27 and 17.59 mmol C m^{-2} d^{-1}. The samplings in Mar-17 and May-18 showed the higher emissions, whereas the samplings in Jun-17 and Nov-17 showed the lower. Considering all the lagoon complex (area-weighted including rivers and lagoons stations), the CO_2 emissions ranged between 9.8 to 70.5 mmol C m^{-2} d^{-1}. For the diffusive emissions of CH_4, the rivers showed extreme high values of degassing, with the magnitudes of emissions being between two and three orders of magnitude higher than those verified in the lagoon stations. The ranges of riverine CH_4 emissions were between 22.58 to 185.12 mmol C m^{-2} d^{-1}. In the lagoons, the emissions ranged between 0.2 to 1.4 mmol C m^{-2} d^{-1}. Considering all the lagoon complex (area-weighted of rivers and lagoons), the CH_4 emissions ranged between 2.2 and 16.5 mmol C m^{-2} d^{-1}.

4.Discussion

4.1.The high concentrations of TA and DIC in hypoxic/anoxic river waters

TA is considered a relative conservative property of natural waters (Kempe 1990; Wolf-Gladrow et al. 2007). In estuaries, TA generally shows a linear distribution versus the salinity exhibiting conservative mixing. However, in coastal regions enriched in organic matter were anaerobic processes are significant, the assumption of conservatively TA can be abusive because the reactions of reduction and oxidation are coupled to proton production and consumption, contributing to changes in TA (Abril and Frankignoulle 2001; Hu and Cai 2011). Indeed, anaerobic decomposition of organic matter by denitrification, reduction of iron and manganese oxides, and sulfate reduction are proton consuming processes that will produce TA and DIC with specific stoichiometric ratios. Table 3 presents the stoichiometry of main chemical reactions involved in generation/consumption of TA in coastal regions. In the polluted rivers of the JLC, it is clear that the permanent hypoxic/anoxic conditions favors the production of TA and DIC in waters and sediments due to the high TA concentrations in the freshwater end-members in almost all sampling campaigns and stations. The exception was verified in the sampling of Jun-2017 that occurred under conditions of high accumulated precipitation when 3 river stations presented low TA, suggesting dilution during rainy conditions. The rivers of the JLC watershed are inserted in a region of low-carbonate minerals, which contributes with very low concentrations of TA (Meybeck and Ragu 2012). The background values of TA in the regions located upstream to the urban influences are low (~ 300-400 $\mu mol\ kg^{-1}$). Considering that freshwater TA concentrations ranged between 572 to 4,022 $\mu mol\ Kg^{-1}$, the contribution of anaerobic processes on generation of TA is estimated at about 30 to 90%. These values are very similar to that found in the polluted Scheldt estuarine basin in the Belgium (Abril and Frankignoulle 2001), where the authors found bicarbonate (HCO_3^-) concentrations 2-10 times higher than the representative concentrations reported in pristine basins. The authors calculated that 22% to 63% of TA concentrations were attributed to process involving nitrogen cycling (ammonification, nitrification and denitrification).

The plot between the deviation from the conservative mixing of TA and DIC (ΔTA and ΔDIC) reveals regions of gains and losses of TA and DIC along the lagoon complex (Fig. 4). Data points from the river stations presented always-positive values, consistent with the production of TA and DIC. The distributions of ΔTA and ΔDIC follows mainly the vectors which represent the processes of carbonate dissolution, sulphate reduction and denitrification (see the figure caption for detailed descriptions, and Tab. 3). Carbonate dissolution is unlikely to occur due to the low concentration of carbonate minerals in the watershed, whereas denitrification and sulphate reduction are likely to occur in a significant way. Overall, the highest concentrations of TA were coincident with the highest concentrations of NH_4^+ (Fig. 3c), possibly reflecting the denitrification process. The exception was verified in Jun-2017, which occurred under high rainy conditions (highest accumulated precipitation before 7 days of sampling), when TA seemed to be diluted and NH_4^+ concentrations still high possibly reflecting the urban runoff. Overall, the rivers of the JLC presented remarkably high NH_4^+ concentrations, in the same order of magnitude verified only in the high polluted Adyar estuary – India (average between 1,200 and 3,000 $\mu mol\ L^{-1}$; Nirmal-Rajkumar et al. 2008), and well above than found in rivers enriched in nitrogen (McMahon and Dennehy 1999). These values are comparable to those found in municipal wastewaters (Hammer and Hammer 2012). Denitrification produces DIC and TA which generates nitrogen (N_2), which in turn escapes to the atmosphere (Abril and Frankignoulle 2001; Thomas et al. 2009). This represents an irreversible generation of TA, because the product resists or escapes re-oxidation by oxygen (Thomas et al. 2009). The same is valid for the sulfate reduction, which generates hydrogen sulfite (H_2S) (Thomas et al. 2009). However, TA, NH_4^+, NO_3^- and DO concentrations in the intermediate salinities suggest that during river-ocean mixing are occurring important processes of re-oxidation that can be a sink for TA compensating the TA generated in the anoxic waters (Hu and Cai 2011; Gustafsson et al. 2019) (see next section of the manuscript).

The aerobic respiration can also contributes to the increases of DIC concentrations in heterotrophic waters (Borges and Abril 2011); however, in these polluted and anoxic riverine stations this process seems to be minor compared to anaerobic/anoxic processes. This can be confirmed by looking at the relationship between E-DIC and AOU (Fig. 5b). The data points of the river stations present strong deviation above the 1:1 line, which represents the theoretical quotient between photosynthesis and respiration. This means that additional processes are contributing to the production of DIC that are not linked to the aerobic microbial respiration. This graph shows that the production of DIC can continue even if the oxygen is depleted. These conditions were verified in high pCO_2 estuaries, and attributed mainly to lateral inputs of dissolved CO_2 and anoxic production in waters and sediments (Cai et al. 1999; Abril et al. 2002; Borges and Abril 2011).

4.2.The carbonate chemistry in the lagoon waters

Contrary to the exposed above for the rivers, the lagoon stations present important losses of TA and DIC along the salinity gradient, with prevalence of negative values of ΔTA and ΔDIC in these more oxygenated waters (Fig. 4). Comparing the covariations of ΔTA and ΔDIC along the salinity gradient, the data points followed mainly the vectors representing the processes of sulphur oxidation, iron oxidation and nitrification that are involved only in the consumption of TA, without net effect on DIC (Abril and Frankignoulle 2001; Baldry et al. 2019; Rassmann et al., 2020). In the lagoons, the mixing of anoxic-acid freshwaters with well-oxygenated waters is associated with processes of re-oxidation of reduced by-products of organic matter degradation, generating titration of TA to dissolved CO_2 particularly evident in the middle salinity regions. These intermediate saline waters (10-20) presented the lowest TA concentrations and well-below than freshwater and marine end-members, coincident with minimum concentrations of NH_4^+, and maximum concentrations of NO_3^- and DO. The nitrification is a process that consumes TA, when NH_4^+ is oxidized to NO_3^-, producing $2H^+$. TA concentrations present an important and inverse relationship with NO_3^- concentrations, corroborating this assumption (Fig. 3b). This suggests that this is an area were nitrification is complete, counter-acting the process of denitrification that occurs in the anoxic freshwaters, compensating the TA generated in anoxic waters. In this way, the lagoon reflects a combination of processes, which are the denitrification and ammonification in anoxic conditions, nitrification in well-oxygenated conditions. Indeed, the complete coupling of ammonification-nitrification-denitrification does not lead to net TA gain (Hu and Cai 2011). In addition, the re-oxidation of all other reduced compounds (H_2S, Fe^{2+}, Mn^{2+}, and also a part of CH_4) is probably also complete. However, it must be stressed that the re-oxidation of reduced species are often complex involving many intermediate steps and side products (Cai et al. 2017). The re-oxidation decreases the TA down to 1,500 μmol kg^{-1}, much lower than the end-members concentrations. Important re-oxidation processes were described in the high-polluted Scheldt basin, when the ecosystem changes from reducing to oxidizing conditions (Abril and Frankignoulle 2001).

The process of primary production is also probably to occur in the mixing zone, with significant changes in DIC concentrations due to the uptake by primary production. Occasional occurrence of phytoplankton blooms were found in the lagoon stations (highest value of Chl *a* of 77 μg L^{-1}), with decreasing concentrations of DIC, and increasing levels of pH and dissolved oxygen. The process of primary production can be strongly stimulated by high availability of nutrients in the water column, shallow depths, high temperature and high incidence of photosynthetically active radiation (Cotovicz et al. 2015). The influence of biological activities on the carbonate chemistry is apparent comparing the E-DIC versus AOU values (Fig. 5b). Positive E-DIC and AOU values suggest that the system is predominant heterotrophic. The regression line between E-DIC and AOU for the lagoon stations (green line) is very close to the line 1:1, suggesting that the processes of gross primary production and total respiration are coupled in the lagoons (but not in the rivers). This was also showed in the Guanabara Bay (Rio de Janeiro, Brazil), an eutrophic coastal embayment dominated by phytoplankton blooms (Cotovicz et al. 2015) and located close to the JLC. However, for JLC other biogeochemical processes described above like denitrification-nitrification and iron reduction-oxidation can also follows closely the 1:1 line (Tab. 3). The biological influences on the carbonate chemistry are also apparent looking at the relationship between O_2 and pH (Fig. 5a). This graph shows a strongly significant and positive relationship between these parameters ($R^2 = 0.94$, $p < 0.0001$). In general, the river stations present very low values of pH coincident with hypoxic/anoxic conditions.

4.3.Spatial distributions of dissolved CO_2 and CH_4 in the JLC

Inner and low-salinity estuarine regions have been documented as heterotrophic and large CO_2 emitters (Frankignoulle et al. 1998; Silvennoinen et al. 2008). In several coastal waters worldwide, important CO_2 changes have been strongly related to eutrophication (Borges and Gypens 2010; Cai et al. 2011; Sunda and Cai 2012; Cotovicz et al. 2015; Brigham et al. 2019). Overall, when untreated urban wastewater discharges from megacities reach estuarine waters, they enhance the levels of CO_2 especially in turbidity coastal waters located at the vicinity of outfalls (Frankignoulle et al. 1998; Zhai et al. 2007; Sarma et al. 2012; Brigham et al. 2019). These characteristics of high pCO_2 values are observed in the polluted rivers that compose the drainage basin of the JLC. The averaged values of pCO_2 in these rivers ranged between 6,838 and 13,641 ppmv. These values were verified only in highly impacted estuaries, i. e., Tapti Estuary – India (Sarma et al. 2012), Scheldt Estuary – Belgium (Frankignoulle et al. 1998), Pearl River – China (Guo et al. 2009). The river waters of the JLC presented an extreme oxygen depletion reaching anoxic conditions in surface waters in almost all stations and sampling campaigns, all related to supersaturation of pCO_2. The wastewater contribution is corroborated by the massive NH_4^+ concentrations reaching concentrations measured in municipal wastewaters (Hammer and Hammer 2012).

Following the seaward direction, the levels of pCO_2 decreases exponentially with the increases of salinity. This decrease is associate with degassing, biogeochemical processes and mixing with low-pCO_2 waters (Cotovicz et al. 2020). The CO_2 degassing is strongest at the freshwater stations, taking account that the dissolved concentrations are at the highest in this estuarine region, creating a steep gradient between the pCO_2 in the air and in the water. The freshwaters enters in the lagoon with highly reduced conditions, but the mixing with more oxygenated waters creates conditions favoring important processes of re-oxidation, as discussed above. The processes of manganese reduction and iron reduction are linked to the production of CO_2 and consumption of TA in transitional oxic/anoxic estuarine regions (Abril and Frankignoulle 2001). In this way, the pCO_2 values reflects both the physical mixing, and the biogeochemical processes. For intermediate to high-salinities the low values of pCO_2 values are expected due to the mixing with low-pCO_2 seawaters (Chen et al. 2013; Cotovicz et al. 2020), taking account that the adjacent coastal waters present pCO_2 averaging 411 ppmv (Cotovicz et al., 2015). The uptake of CO_2 by primary producers are likely to occur since that phytoplankton blooms occurred in some stations, and also attributed to this marked decline of pCO_2. Overall, pCO_2 values did not present a clear seasonal tendency; however the lowest average of pCO_2 in the rivers were found in June-2017, when the accumulated precipitation of 7 days was at highest levels, probably associate with dilution.

Approaching the behavior generally found for CO_2, CH_4 concentrations are often much greater in the uppermost portion of estuaries (Upstill-Goddard et al. 2000; Middelburg et al. 2002; Upstill-Goddard and Barnes 2016). The methanogenesis is a process of organic matter degradation that is favored when all the other proton acceptors are depleted (i.e., nitrate, sulphate, manganese), occurring in hypoxic/anoxic conditions. High CH_4 concentrations are frequently found in water and wastewater throughout integrated urban drainage systems composed of sewer systems, wastewater treatment plants and receiving water bodies (Nirmal-Rajkumar et al. 2008; Yu et al., 2017). The primary methanogenic pathways are the conversion of acetate to CO_2 and CH_4, and reduction of CO_2 with H_2 (Whitman et al. 1992; Matson and Harriss 2009). In severely impacted estuaries, the CH_4 concentrations can span several orders of magnitude spatially and temporally (Nirmal-Rajkumar et al. 2008; Burgos et al. 2015; Cotovicz et al. 2016). The concentrations of dissolved CH_4 found in surface waters of JLC are very high, with an extreme maximum of 288,572 nmol L^{-1} in the river zone. To our best knowledge, this is the second highest concentration measured for any natural river–estuarine system, only behind that measured in the Adyar Estuary (maximum of 386,000 nmol L-1; Nirmal-Rajkumar et al. 2008). Indeed, a study proposed a rank of averaged dissolved CH_4 concentrations in estuarine environments (Cotovicz et al. 2016). Updating this rank, the waters of JLC presented, on average, the second highest CH_4 estuarine water concentrations worldwide (average of 976 nmol L^{-1}). Only strongly polluted estuaries occupy the other firsts positions: Adyar Estuary – India (2,200 nmol L-1; Nirmal Rajkumar et al. 2008), Guadalete Estuary – Spain (590 nmol L-1; Burgos et al. 2015) and Guanabara Bay – Brazil (456 nmol L-1; Cotovicz et al. 2016). The anthropogenic-derived organic carbon in the JLC is likely to be massive taking account that the watershed hosts a huge population and the wastewater treatment covers less than 30% of the total households. The levels of accumulated precipitation were not correlated to the concentrations of CH_4, however, highest concentrations were observed in Nov-2017 (when the accumulated precipitation of 7 days before sampling was low), preventing the dilution by rain water. Heavy rain events could occur in the region, with possibility to alter the CO_2 and CH_4 concentrations. Climatological and hydrological effects on GHG dynamics needs further investigation.

There was a positive correlation between pCO_2 and CH_4 in all campaigns, suggesting a common source of these two gases (Fig. 6). However, for similar pCO_2 values, the concentrations of CH_4 were higher, spanning until one order of magnitude. This was also showed in other estuaries, for example described in tropical mangrove-dominated estuaries of Australia, where the authors attributed this pattern to a mosaic of processes, including the presence of sewage treatment plants, differential groundwater and riverine carbon inputs, and exchange with vegetated coastal habitats (Rosentreter et al. 2018). In JLC, the high presence of untreated domestic effluent discharges associated with strong oxygen depletion seems to enhance disproportionally the production of CH_4 compared to CO_2, particularly in the sampling in Nov-17. According to the analysis of Borges and Abril (2011), and after updated by Cotovicz et al. (2016), there is a positive relationship between CH_4 and pCO_2 in well-mixed estuarine systems, and a marked negative relationship in stratified estuarine systems. In well mixed systems, CH_4 and CO_2 present a positive tendency due to degradation of allochtonous organic matter in soils and sediments that are then transported to the estuary, i. e., CO_2 and CH_4 present a same origin. In stratified systems the relationship is negative because the autochthonous organic matter is produced by primary producers in surface waters, lowering the pCO_2. The produced organic matter is further transferred across the pycnocline and promoting anoxic conditions in bottom layers due to organic matter degradation, favoring the methanogenesis in bottom water and sediments (Fenchel et al. 1995; Koné al. 2010). This produced CH_4 is further transported to

surface water by advection and diffusion, turning the surface waters enriched in CH_4. However, these tendencies seems to be "perturbed" in anoxic and organic-rich coastal waters, when the CH_4 production is disproportionally favored.

4.4.Diffusive emissions of CO_2 and CH_4

According to the most recent global compilation of estuarine CO_2 emissions propose by Chen et al. (2013), upper estuaries are sources of CO_2 on the order of 106 mmol C m^{-2} d^{-1}, mid-estuaries emit 47 mmol C m^{-2} d^{-1} , and lower estuaries with salinities more than 25 are sources of 23 mmol C m^{-2} d^{-1}. Considering all JLC, the emissions ranged between 22.00 to 48.67 mmol m^{-2} d^{-1}. In this way, the CO_2 emissions in the JLC are very close to the ranges estimated in other estuaries. However, considering only the river stations, the CO_2 outgassing ranged between 199 to 435 mmol C m^{-2} d^{-1}. These values are between 2 to 4-fold higher than the averaged emissions of CO_2 by freshwaters and low salinity regions of estuaries. Emissions on this order of magnitude were found only in high-impacted estuaries and carbon-rich environments, for example, in the Cochin Estuary - India (267 mmol C m^{-2} d^{-1}; Gupta et al. 2009); Douro, Elbe, Loire, Scheldt, and Sado - European Estuaries (between 155 and 396 mmol C m^{-2} d^{-1}; Frankignoulle et al. 1998; Abril et al. 2003); Potou lagoon - Ivory Coast (186.0 mmol C m^{-2} d^{-1}; Koné et al 2009); Tapti Estuary – India (362 mmol C m^{-2} d^{-1}; Sarma et al. 2012).

The air-water CH_4 fluxes to the atmosphere are strongly related to typology of coastal ecosystems, and also the degree of human influence. Concerning diffusion only, the air-water CH_4 fluxes ranges from 0.04 ± 0.17 mmol C m^{-2} d^{-1} for coastal plumes to 1.85 ± 0.99 mmol C m^{-2} d^{-1} for fjords and coastal lagoons, with intermediate values for low salinity zones, marsh and mangrove creeks (Borges and Abril 2011). Considering the ecosystem as a whole, the JLC presented emissions varying between 2.19 to 16.47 mmol m^{-2} d^{-1}, which are among the highest documented in estuaries worldwide. The CH_4 emissions on this order of magnitude were found only in high-impacted ecosystems, for example, in the Adyar Estuary – India (4.70 mmol m^{-2} d^{-1}; Nirmal-Rajkumar et al. 2008); Coastal Lagoon of the Ivory Coast (2.40 mmol m^{-2} d^{-1}; Koné et al. 2010) and Guanabara Bay – Brazil (0.24 to 4.79 mmol m^{-2} d^{-1}; Cotovicz et al. 2016). The average flux intensities in the JLC are between two and three order of magnitude higher than values normally found in shelf waters (~0.03 mmol m^{-2} d^{-1}) and between four and five orders of magnitude higher than values of the open ocean waters (~0.0004 mmol m^{-2} d^{-1}) (Borges et al. 2016).

We used the global warming potential (GWP) and CO_2-equivalent emissions (CO_2-eq) (IPCC 2013) to compare the fluxes of CH_4 with those of CO_2. This metric was calculated with the gas transfer velocity of RC01. After converting to CO_2-eq, the emissions of CO_2 ranged between 1.11 to 2.94 g CO_2-eq m^{-2} d^{-1}. For CH_4 the CO_2-eq emissions ranged between 2.17 to 6.11 g CO_2-eq m^{-2} d^{-1} (Tab. 4). Expressed as CO_2-eq, CH_4 accounted for a major portion of the GHG warming potential in the lagoon (between 46% to 80%) especially in the river stations where the CH_4 was always more important than CO_2. This is unusual since that normally CO_2 is the main GHG in aquatic coastal ecosystems (Campeau et al. 2014; Sadat-Noori et al. 2018). However, studies have suggested that CH_4 can be the main source of CO_2-eq emissions in smaller streams of fluvial network and mangrove ecosystems (Campeau et al. 2014; Sea et al. 2018). Now, we are showing that in extremely impacted ecosystem the CH_4 is the most important GHG in terms of CO_2eq. This study quantified only the diffusive emissions of CH_4, however coastal areas ensures several pathways of CH_4 to the atmosphere, including the ebullition. Ebullition is probable to occur in the JLC, since that the threshold value of $5x10^4$ nmol L^{-1} of dissolved CH_4 beyond which bubbles can forms in aquatic sediments (Chanton et al. 1989) was regularly surpassed in the polluted rivers. Bubble evasion from the surface waters was visually observed in the river stations, which could make CH_4 contribution even stronger.

5.Conclusions

Our study reveals some of the biogeochemical processes that occur in the case of strongly polluted rivers discharging to coastal lagoons, with considerable effects on carbonate chemistry and emissions of CO_2 and CH_4 to the atmosphere. The rivers that compose the watershed are highly polluted, presenting quasi-permanent situations of oxygen depletion. These rivers receive large amounts of anthropogenic-derived organic matter, mostly from domestic effluents, that are discharged "*in natura*" in the waters. This large amount of fresh organic matter contributes to strong oxygen consumption linked to the intense heterotrophic activities reaching conditions of hypoxia and anoxia. Anaerobic processes such as denitrification and sulphate reduction are intrinsically coupled to the transfer of protons, which favor the production of TA. These processes also

contribute with production of DIC. The calculated emissions of CO_2 and CH_4 in these polluted rivers are among the highest documented in coastal waters.

For the lagoon stations, the deviation from the conservative mixing suggested that additional processes are taking place along the river-ocean continuum. The concentrations of TA, DIC, CO_2 and CH_4 decreased substantially from the rivers to the lagoon waters. The decreases of TA and DIC are attributed to re-oxidation processes such as sulphur oxidation, iron oxidation and nitrification during the mixing of anoxic freshwaters with oxic estuarine waters. The marked decreases of DIC concentrations are also attributed to air-water exchanges (CO_2 outgassing), and primary production. The lagoon waters remains with CO_2 oversaturated conditions, however, the growth of large phytoplankton blooms contributed with occasional conditions of subsaturation, associated with high DO and pH. For CH_4, the main processes are the mixing with low-CH_4 seawaters, degassing and CH_4 oxidation. Considering only the lagoon stations, the CO_2 emissions are on the same order of magnitude verified in other ecosystems worldwide, however, for the CH_4 these emissions are among the highest already reported.

Compared in terms of CO_2eq, the CH_4 emissions were most important than CO_2, suggesting that ecosystems strongly polluted by anthropogenic-derived organic carbon produces more CH_4 comparatively to CO_2, especially under strong oxygen depletion. These results confirm that severely polluted and eutrophicated coastal lagoons are hotspot of GHG emissions. Therefore, global carbon budgets assertions in coastal regions must include these eutrophicated areas in order to increase the reliability of the proposed estimates. In addition, urgent actions are needed with purposes to reduce the eutrophication in urban coastal ecosystems, in order to mitigate the climate change and to improve the ecosystem health.

Declarations

Ethics approval and consent to participate: Not applicable

Consent for publication: Not applicable

Availability of data and materials: The datasets used and/or analysed during the current study are available from the corresponding author on reasonable request.

Competing interests: The authors declare that they have no competing interests.

Funding: Carlos Chagas Foundation for Research Support of the State of Rio de Janeiro (FAPERJ; proc. no. E-26202.785/2016).

Authors' contributions: LCCJr: Conceptualization, Coordination, Execution, Data curation, Formal analysis, Methodology, Writing - original draft. RPR: Laboratorial Analysis, Writing – review. LOV, CRR, DT: Execution, Laboratorial Analysis. MB, RS: Conceptualization, Execution, Writing – review. BAK: Conceptualization, Funding acquisition, Supervision, Writing – review. GA: Conceptualization, Data curation, Formal analysis, Methodology, Supervision, Writing - original draft.

Acknowledgments

This study was supported by the Carlos Chagas Foundation for Research Support of the State of Rio de Janeiro (FAPERJ; proc. no. E- 26202.785/2016), and by the Coordination for the Improvement of Higher Education Personnel (CAPES). Luiz C. Cotovicz Jr. thanks the UFC-PRPPG for a visiting professor grant at the Marine Sciences Institute (LABOMAR).

Figure Captions

Fig. 1 Map showing the localization of the Jacarepagua Lagoon Complex (JLC). The red squares represent the locations of river stations. The green squares represent the locations of lagoon stations. The yellow line represents the contour of the lagoons and the rivers. The orange line refers to an ecological barrier that impedes the navigation in the landward direction.

Fig. 2 Distributions of the main parameters analyzed in this study along the salinity gradient. The red circles represent the river stations, whereas the green circles represent the lagoon stations.

Fig. 3 Scatter plots between: a) NH_4^+ and O_2; b) NO_3^- and O_2; c) NH_4^+ and TA; d) NO_3^- and TA including all stations and sampling campaigns.

Fig. 4 Deviations from conservative mixing lines of TA (ΔTA) as a function of DIC (ΔDIC) in the river stations (red dots) and lagoon stations (green dots), for all sampling campaigns. The unitless directional vectors representing the slopes of the following processes: (1) iron reduction; (2) carbonate dissolution; (3) sulphate reduction; (4) denitrification; (5) CO_2 influx (ingassing); (6) aerobic respiration; (7) sulphur pxidation, iron oxidation and nitrification; (8) carbonate precipitation, (9) CO_2 efflux (degassing); (9) primary production.

Fig. 5 Graph a) shows the relationship between pH and O_2, for all sampling campaigns. The black line represents the linear regressions. Graph b) shows the relationship between the excess dissolved inorganic carbon (E-DIC) and apparent utilization of oxygen (AOU). The 1:1 black line represents the quotient between CO_2 and O_2 during the processes of photosynthesis and respiration. The green line represents the linear regressions considering only the lagoon stations. Graph c) shows the relationship between the concentrations of CH_4 and apparent utilization of oxygen (AOU). Note that the y-axis is logarithmic. Red dots are the station in the rivers, and green dots are the stations in the lagoons.

Fig. 6 CH_4 dissolved concentrations vs. average partial pressure of CO_2 (pCO_2) for the sampling campaigns in Mar-2017, Jun-2017 and Nov-2017. For the Mar-2017 the blue line represents the linear regressions. For Mar-2017 and Nov-2017 the relationship showed a linear tendency, whereas for Jun-2017 the relationship followed a non-linear trend, fitting in an exponential growth.

References

Abril G, Frankignoulle M (2001) Nitrogen – alkalinity interactions in the highly polluted Scheldt Basin (Belgium). Water Res 35: 844–850. https://doi.org/10.1016/S0043-1354(00)00310-9

Abril G, Iversen N (2002) Methane dynamics in a shallow, non-tidal, estuary (Randers Fjord, Denmark). Mar Ecol Prog Ser 230:171–181. https://doi.org/10.3354/meps230171

Abril G, Etcheber H, Delille B, Frankignoulle M, Borges AV (2003) Carbonate dissolution in the turbid and eutrophic Loire estuary. Mar Ecol Prog Ser 259:129–138. https://doi.org/10.3354/meps259129

Abril G, Commarieu MV, Guerin F (2007) Enhanced methane oxidation in an estuarine turbidity maximum. Limnol Oceanogr 52:470–475. https://doi.org/10.4319/lo.2007.52.1.0470

Abril G, Martinez J-M, Artigas LF, Moreira-Turcq P, Benedetti MF, Vidal L, Meziane T, Kim J-H, Bernardes MC, Savoye N, Deborde J, Albéric P, Souza MFL, Souza EL, Roland F (2014) Amazon River Carbon Dioxide Outgassing fueled by Wetlands. Nature 505:395–398. https://doi.org/10.1038/nature12797

Amarante, OA, Silva FJ, Rios Filho L G (2002) Wind power atlas of the Rio de Janeiro State. Secretaria de Estado da Energia da Indústria Naval e do Petróleo, Rio de Janeiro. (in Portuguese) http://www.cresesb.cepel.br/publicacoes/download/atlas_eolico/AtlasEolicoRJ.pdf. Accessed 27 April 2018

ANA 2019. Water National Agency. Natiotal atlas of sewage: De-pollution of river basins. (in Portuguese) http://www.snirh.gov.br/portal/snirh/snirh-1/atlas-esgotos. Accessed 25 January 2020

Baldry K, Saderne V, McCorkle D, Churchill JH, Agusti S, Duarte C (2019) Anomalies in the Carbonate System of Red Sea Coastal Habitats. Biogeosciences 17:423-439. https://doi.org/10.5194/bg-17-423-2020

682 Bange H W (2006) Nitrous oxide and methane in European coastal waters. Estuar Coast Shelf Sci 70: 361–374.
683 https://doi.org/10.1016/j.ecss.2006.05.042

684 Benson BB, Krause D (1984) The concentration and isotopic fractionation of oxygen dissolved in freshwater and
685 seawater in equilibrium with the atmosphere. Limnol Oceanogr 29:620–632.
686 https://doi.org/10.4319/lo.1984.29.3.0620

687 Borges AV, Gypens N (2010) Carbonate chemistry in the coastal zone responds more strongly to eutrophication
688 than to ocean acidification. Limnol Oceanogr 55:346-353. https://doi.org/10.4319/lo.2010.55.1.0346

689 Borges AV, Abril G (2011) Carbon dioxide and methane dynamics in estuaries. In: McLusky D, Wolanski E
690 (eds) Treatise on Estuarine and Coastal Science. Academic Press, Amsterdam, pp 119–161.
691 https://doi.org/10.1016/B978-0-12-374711-2.00504-0

692 Borges AV, Abril G, Darchambeau F, Teodoru CR, Deborde J, Vidal LO, Lambert T, Bouillon S (2015)
693 Divergent biophysical controls of aquatic CO_2 and CH_4 in the World's two largest rivers. Sci Rep 5 :1–10.
694 https://doi.org/10.1038/srep15614

695 Borges AV, Champenois W, Gypens N, Delille B, Harlay J (2016) Massive marine methane emissions from
696 near-shore shallow coastal areas. Sci Rep 6:27908. https://doi.org/10.1038/srep27908

697 Bricker SB, Longstaff B, Dennison W, Jones A, Boicourt K, Wicks C, Woerner J (2008) Effects of nutrient
698 enrichment in the nation's estuaries: A decade of change. Harmful Algae. 8:623 21-32.
699 https://doi.org/10.1016/j.hal.2008.08.028

700 Brigham BA, Bird JA, Juhl AR, Zappa CJ, Montero AD, O'Mullan GD (2019) Anthropogenic inputs from a
701 coastal megacity are linked to greenhouse gas concentrations in the surrounding estuary. Limnol Oceanogr
702 64:2497-2511. https://doi.org/10.1002/lno.11200

703 Burgos M, Sierra A, Ortega T, Forja JM (2015) Anthropogenic effects on greenhouse gas (CH4 and N2O)
704 emissions in the Guadalete River Estuary (SW Spain). Sci Total Environ 503–504: 179–189.
705 https://doi.org/10.1016/j.scitotenv.2014.06.038

706 Cai W-J, Pomeroy LR, Moran MA, Wang Y (1999) Oxygen and carbon dioxide mass balance for the estuarine–
707 intertidal marsh complex of five rivers in the southeastern U.S. Limnol Oceanogr 44:639-649.
708 https://doi.org/10.4319/lo.1999.44.3.0639

709 Cai W-J, Hu X, Huang W, Murrell MC, Lehrter JC, Lohrenz SE, Chou W, Zhai W, Hollibaugh JT, Wang Y,
710 Zhao P, Guo X, Gundersen K, Dai M, Gong G (2011) Acidification of Subsurface Coastal Waters Enhanced by
711 Eutrophication. Nature Geoscience 4, 766-770. http://dx.doi.org/10.1038/NGEO1297.

712 Cai W-J, Huang W-J, Luther GW, Pierrot D, Li M, Testa J, Xue M, Joesoef A, Mann R, Brodeur J, Xu Y-Y,
713 Chen B, Hussain N, Waldbusser GG, Cornwell J, Kemp WM (2017) Redox reactions and weak buffering
714 capacity lead to acidification in the Chesapeake Bay. Nat Commun 8 :369. https://doi.org/10.1038/s41467-017-
715 00417-7

716 Campeau A, Lapierre J-F, Vachon D, del Giogio P A (2014) Regional contribution of CO_2 and CH_4 fluxes from
717 the fluvial network in a lowland boreal landscape of Québec. Global Biogeochem Cy 28: 57–69.
718 https://doi.org/10.1002/2013GB004685

719 Chanton JP, Martens CS, Kelley CA (1989) Gas transport from methane saturated, tidal freshwater and wetland
720 sediments. Limnol Oceanogr 34:807–819. https://doi.org/10.4319/lo.1989.34.5.0807

721 Chen CT, Huang TH, Chen YC, Bai Y, He X, Kang Y (2013) Air–sea exchanges of CO_2 in the world's coastal
722 seas. Biogeosciences 10:6509–6544. https://doi.org/10.5194/bg-10-6509-2013

723 Cotovicz LC, Knoppers BA, Brandini N, Costa Santos SJ, Abril G (2015) A strong CO_2 sink enhanced by
724 eutrophication in a tropical coastal embayment (Guanabara Bay, Rio de Janeiro, Brazil). Biogeosciences
725 12:6125–6146. http://doi.org/10.5194/bg-12-6125-2015.

726 Cotovicz LC, Knoppers BA, Brandini N, Poirier D, Costa Santos SJ, Abril G (2016) Spatio-temporal variability
727 of methane (CH4) concentrations and diffusive fluxes from a tropical coastal embayment surrounded by a large

urban area (Guanabara Bay, Rio de Janeiro, Brazil). Limnol Oceanogr 61:S238–S252. http://doi.org/10.1002/lno.10298.

Cotovicz LC, Knoppers BA, Brandini N, Poirier D, Costa Santos SJ, Abril G (2018) Aragonite saturation state in a tropical coastal embayment dominated by phytoplankton blooms (Guanabara Bay - Brazil). Mar Pollut Bull 129: 729-739. https://doi.org/10.1016/j.marpolbul.2017.10.064

Cotovicz LC, Vidal LO, de Rezende CE, Bernardes MC, Knoppers BA, Sobrinho RL, Cardoso RP, Muniz M, dos Anjos RM, Biehler A, Abril G (2020) Carbon dioxide sources and sinks in the delta of the Paraíba do Sul River (Southeastern Brazil) modulated by carbonate thermodynamics, gas exchange and ecosystem metabolism during estuarine mixing. Mar Chem. https://doi.org/10.1016/j.marchem.2020.103869

De-Magalhães L, Noyma N, Furtado LL, Mucci M, van Oosterhout F, Huszar VLM, Marinho MM, Lürling M (2017) Efficacy of coagulants and ballast compounds in removal of cyanobacteria (Microcystis) from water of the tropical lagoon Jacarepaguá (Rio de Janeiro, Brazil). Estuar Coast 40:121–133. https://doi.org/10.1007/s12237-016-0125-x.

Dickson AG, Millero FJ (1987) A comparison of the equilibrium constants for the dissociation of carbonic acid in seawater media. Deep-Sea Res 34:1733–1743. https://doi.org/10.1016/0198-0149(87)90021-5

Dickson AG (1990) Standard potential of the reaction: $AgCl(s) + 1/2H_2(g) = Ag(s) + HCl(aq)$, and the standard acidity constant of the ion HSO_4 in synthetic sea water from 273.15 to 318.15 K. J. Chem Thermodyn 22:113-127. https://doi.org/10.1016/0021-9614(90)90074-Z

Etheridge DM, Steele LP, Francey RJ, Langenfelds RL (1998) Atmospheric methane between 1000 A.D. and present: Evidence of anthropogenic emissions and climatic variability. J Geophys Res 103:15979-15993. https://doi.org/10.1029/98JD00923

Frankignoulle M, Abril G, Borges A, Bourge I, Canon C, Delille B, Libert E, Theate J M (1998) Carbon Dioxide Emission from European Estuaries. Science 282 :434–436. https://doi.org/10.1126/science.282.5388.434

Gomes AM, Sampaio P, Ferrão-Filho A, Magalhães VF, Marinho MM, Oliveira AC, Santos V, Domingos P, Azevedo SM (2009) Toxic cyanobacterial blooms in an eutrophicated coastal lagoon in Rio de Janeiro, Brazil: Effects on human health. Oecol Bras 13:329-345.

Gran G (1952) Determination of the equivalence point in potentiometric titrations-part II. Analyst 77:661–671.

Grasshoff K, Ehrhardt M, Kremling K (1999) Methods of Seawater Analysis, 3rd edition, Wiley-VCH, Weinhein.

Guérin F, Abril G, Serça D, Delon C, Richard S, Delmas R, Tremblay A Varfalvy L (2007) Gas transfer velocities of CO_2 and CH_4 in a tropical reservoir and its river downstream. J Mar Syst 66 :161–172. https://doi.org/10.1016/j.jmarsys.2006.03.019

Guo X, Dai M, Zhai W, Cai W-J, Chen B (2009) CO_2 flux and seasonal variability in a large subtropical estuarine system, the Pearl River Estuary, China. J Geophys Res 114:G03013. https://doi.org/10.1029/2008JG000905

Gupta GVM, Thottathil SD, Balachandran KK, Madhu NV, Madeswaran P, Nair S (2009) CO_2 Supersaturation and Net Heterotrophy in a Tropical Estuary (Cochin, India): Influence of Anthropogenic Effect. Ecosystems 12:1145–1157. https://doi.org/10.1007/s10021-009-9280-2

Hammer MJ, Hammer MJ (2012) Water and wastewater technology. Prentice Hall, Pearson Education Inc., NJ, USA.

Howarth R, Chan F, Conley DJ, Garnier J, Doney SC, Marino R, Billen G (2011) Coupled biogeochemical cycles: eutrophication and hypoxia in temperate estuaries and coastal marine ecosystems. Frontiers in Ecology and the Environment. 9: 18-26. https://doi.org/10.1890/100008

Hu X, Cai W-J (2011) An assessment of ocean margin anaerobic processes on oceanic alkalinity budget. Global Biogeochem Cy 25:GB3003. https://doi.org/10.1029/2010GB003859

IPCC 2013. Climate Change 2013: The Physical Science Basis. Contribution of Working Group I to the Fifth Assessment Report of the Intergovernmental Panel on Climate Change. In: Stocker TF et al. (eds.) Cambridge Univ. Press. https://doi.org/10.1017/CBO9781107415324

Jähne B, Munnich KO, Bosinger R, Dutzi A, Huber W, Libner P (1987) On parameters influencing air-water exchange. J Geophys Res 92: 1937–1949. https://doi.org/10.1029/JC092iC02p01937.

Jiang L-Q, Cai W-J, Wang Y (2008) A comparative study of carbon dioxide degassing in river- and marine-dominated estuaries. Limnol Oceanogr 53: 2603–2615. https://doi.org/10.4319/lo.2008.53.6.2603

Kelley CA, Martens CS, Chanton JP (1990) Variations in sedimentary carbon remineralization rates in the White Oak River estuary, North Carolina. Limnol Oceanogr 35:372–383. https://doi.org/10.4319/lo.1990.35.2.0372

Kempe S (1990) Alkalinity: the link between anaerobic basins and shallow water carbonates? Naturwissenschaffer 7:426-427. https://doi.org/10.1007/BF01135940

Kjerfve B (1985) Comparative oceanography of coastal lagoons. In: Wolfe DA (ed) Academic, New York, pp 63–81

Koné YJM, Abril G, Kouadio KN, Delille B, Borges AV (2009) Seasonal Variability of Carbon Dioxide in the Rivers and Lagoons of Ivory Coast (West Africa). Estuar Coast 32:246–260. https://doi.org/10.1007/s12237-008-9121-0

Koné YJM, Abril G, Delille B, Borges AV (2010) Seasonal variability of methane in the rivers and lagoons of Ivory Coast (West Africa). Biogeochemistry 100:21-37. https://doi.org/10.1007/s10533-009-9402-0

Knoppers BA, Carmouze JP, Moreira-Turcqo PF (1999) Nutrient dynamics, metabolism and eutrophication of lagoons along the east Fluminense coast, state of Rio de Janeiro, Brazil. In: Knoppers BA, Bidone ED, Abrão JJ (eds) Environmental geochemistry of coastal lagoon systems of Rio de Janeiro, Brazil. Programa de Geoquímica Ambiental, FINEP, UFF, Rio de Janeiro, pp. 123–154.

Kubo A, Maeda Y, Kanda J (2017) A significant net sink for CO_2 in Tokyo Bay. Sci Rep 7:44355. https://doi.org/10.1038/srep44355

Lee K, Kim, T.W., Byrne, R. H., Millero, F. J., Feely, R. A., Liu, Y.M., 2010. The universal ratio of boron to chlorinity for the North Pacific and North Atlantic oceans, Geochim. Cosmochim. Ac., 74, 1801–1811. https://doi.org/10.1016/j.gca.2009.12.027

Lorenzen C (1967) Determination of chlorophyll and pheo-pigments: spectrophomometric equations. Limnol Oceanogr 12:343-346. https://doi.org/10.4319/lo.1967.12.2.0343

Martens CS, Klump JV (1980) Biogeochemical cycling in an organic-rich coastal marine basin—I. Methane sediment– water exchange processes. Geochim Cosmochim Acta 44: 471–490. https://doi.org/10.1016/0016-7037(80)90045-9

Martens CS, Albert DB, Alperin MJ (1998) Biogeochemical processes controlling methane in gassy coastal sediments—part 1. A model coupling organic matter flux to gas production, oxidation and transport. Cont Shelf Res 18:1741–1770. https://doi.org/10.1016/S0278-4343(98)00056-9

Matson PA, Harriss RC (2009) Biogenic trace gases: measuring emissions from soil and water. Blackwell Science, Oxford

McMahon PB, Dennehy KF (1999) N_2O emissions from a nitrogen enriched river. Environ Sci Technol 33:21-25. https://doi.org/10.1021/es980645n

Mehrbach C, Cuberson CH, Hawley JE, Pytkowicz RM (1973) Measurements of the apparent dissociation constants of carbonic acid in seawater at atmospheric pressure. Limnol Oceanogr 18:897–907. https://doi.org/10.4319/lo.1973.18.6.0897

Meybeck M, Ragu A (2012) GEMS-GLORI world river discharge database. Laboratoire de Géologie Appliquée, Université Pierre et Marie Curie, Paris, France, PANGAEA. https://doi.org/10.1594/PANGAEA.804574

817 Middelburg JJ, Nieuwenhuize J, Iversen N, Hoegh N, de Wilde H, Helder W, Seifert R, Christof O (2002)
818 Methane distribution in European tidal estuaries. Biogeochemistry 59:95–119.
819 https://doi.org/10.1023/A:1015515130419

820 Nirmal-Rajkumar A, Barnes J, Ramesh R, Purvaja R, Upstill-Goddard RC (2008) Methane and nitrous oxide
821 fluxes in the polluted Adyar River and estuary, SE India. Mar Pollut Bull 56:2043–2051. https://doi.org/10.1016/
822 j.marpolbul.2008.08.005

823 Nixon SW (1995) Coastal marine eutrophication: A definition, social causes, and future concerns. Ophelia
824 41:199-219. https://doi.org/10.1080/00785236.1995.10422044

825 NOAA 2019. National Oceanic and Atmospheric Administration. Earth System Research Laboratory. Global
826 Monitoring Division. https://www.esrl.noaa.gov/gmd/ccgg/trends/monthly.html Accessed 20 June 2020

827 Purvaja R, Ramesh R (2000) Human impacts on methane emissions from mangrove ecosystems in India. Reg
828 Environ Change 1 :86-97. https://doi.org/10.1007/PL00011537

829 Rassmann J, , Eitel EM, Lansard B, Cathalot C, Brandily C, Taillefert M, Rabouille C (2020) Benthic alkalinity
830 and dissolved inorganic carbon fluxes in the Rhône River prodelta generated by decoupled aerobic and anaerobic
831 processes. Biogeosciences 17:13-33. https://doi.org/10.5194/bg-17-13-2020

832 Raymond PA, Cole JJ (2001) Gas exchange in rivers and estuaries: Choosing a gas transfer velocity. Estuaries
833 24:312–317. https://doi.org/10.2307/1352954

834 Richey J, Devol A, Wofsy S, Victoria R, Ribeiro M (1988) Biogenic gases and the oxidation and reduction of
835 carbon in Amazon River and floodplain waters. Limnol Oceanogr 33:551-561.
836 https://doi.org/10.4319/lo.1988.33.4.0551

837 Robbins LL, Hansen ME, Kleypas JA, Meylan SC (2010) CO_2 Calc: a user-friendly seawater carbon calculator
838 for Windows, Max OS X, and iOS (iPhone), U.S. Geological Survey Open-File Report, 2010–1280, 1–17.
839 http://pubs.usgs.gov/of/2010/1280/. Accessed 25 February 2019

840 Rosetrenter J, Maher DT, Erler DV, Murray R, Eyre BD (2018) Factors controlling seasonal CO_2 and CH_4
841 emissions in three tropical mangrove-dominated estuaries in Australia. Estuar Coast Shelf S 215:69–82.
842 https://doi.org/10.1016/j.ecss.2018.10.003

843 Sadat-Noori M, Tait D, Maher D, Holloway C, Santos I (2018) Greenhouse gases and submarine groundwater
844 discharge in a Sydney Harbour embayment (Australia). Estuar Coast Shelf S 31: 499-509.
845 https://doi.org/10.1016/j.ecss.2017.05.020

846 Salloto GRB, Cardoso AM, Coutinho FH, Pinto LH, Vieira RP, Chaia C, Lima JL, Albano RM, Martins OB,
847 Clementino MM (2012) Pollution Impacts on Bacterioplankton Diversity in a Tropical Urban Coastal Lagoon
848 System. PLoS One 7:1–12. https://doi.org/10.1371/journal.pone.0051175

849 Samanta S, Dalai TK, Pattanaik JK, Rai SK, Mazumdar A (2015) Dissolved inorganic carbon (DIC) and its
850 δ13C in the Ganga (Hooghly) River estuary, India: evidence of DIC generation via organic carbon degradation
851 and carbonate dissolution. Geochem Cosmochim Acta 165: 226–248. https://doi.org/10.1016/j.gca.2015.05.040.

852 Sampaio, G.F., 2008. Cianobactérias como parâmetros de qualidade ambiental: um estudo do Complexo Lagunar
853 de Jacarepagua. Dissertation, Universidade do Estado do Rio de Janeiro

854 Santos Neves OM, Strauch JC, Ajara C (2017) Dasymetric methods applied to Jacarepagua watershed. Bull
855 Geod Sci 23:606-622. https://doi.org/10.1590/S1982-21702017000400040

856 Sarma VVSS, Viswanadham R, Rao GD et al. (2012) Carbon dioxide emissions from Indian monsoonal
857 estuaries. Geophys. Res. Lett. 39: L03602. https://doi.org/10.1029/2011GL050709

858 Sea M, Garcias-Bonet N, Saderne V, Duarte C (2018) Carbon dioxide and methane fluxes at the air–sea interface
859 of Red Sea mangroves. Biogeosciences 15:5365–5375. https://doi.org/10.5194/bg-15-5365-2018

860 Siegenthaler U, Stocker TF, Monnin E et al. (2005) Stable carbon cycle–climate relationship during the late
861 Pleistocene. Science 25: 1313-1317. https://doi.org/10.1126/science.1120130

Silvennoinen H, Liikanen A, Rintala J, Martikainen PJ (2008) Greenhouse gas fluxes from the eutrophic Temmesjoki River and its Estuary in the Liminganlahti Bay (the Baltic Sea). Biogeochemistry 90:193–208. https://doi.org/10.1007/s10533-008-9244-1

Sunda WG, Cai W-J (2012) Eutrophication induced CO_2-acidification of subsurface coastal waters: interactive effects of temperature, salinity, and atmospheric PCO_2. Environ Sci Technol 46:10651–9. https://doi.org/10.1021/es300626f

Thomas H, Schiettecatte L, Suykens K, Kon YJM (2009) Enhanced ocean carbon storage from anaerobic alkalinity generation in coastal sediments. Biogeosciences 6:267–274. https://doi.org/10.5194/bg-6-267-2009

Upstill-Goddard RC, Barnes J, Frost T, Punshon S, Owens NJP (2000) Methane in the Southern North Sea: Low salinity inputs, estuarine removal and atmospheric flux. Global Biogeochem Cy 14:1205–1217. https://doi.org/10.1029/1999GB001236

Upstill-Goddard RC, Barnes, J (2016) Methane emissions from UK estuaries: Re-evaluating the estuarine source of tropospheric methane from Europe. Mar. Chem. 180, 14–23. doi:10.1016/j.marchem.2016.01.010

Wallace, Y. M. 2005. Guidelines for Estimating Sewage Flows for Sewage Infrastructure Planning. Technical Report No.: EPD/TP 1/05. Environmental Protection Department. Hong Kong. https://www.epd.gov.hk/epd/sites/default/files/epd/english/environmentinhk/water/guide_ref/files/gesf.pdf Accessed 10 March 2019

Wanninkhof R (1992) Relationship between gas exchange and wind speed over the ocean. J Geophys Res 97: 7373–7382. https://doi.org/10.1029/92JC00188

Weiss RF (1974) Carbon dioxide in water and seawater: the solubility of a non-ideal gas. Mar Chem 2: 203–215. https://doi.org/10.1016/0304-4203(74)90015-2

Whitman WB, Bowen TI, Boone DR (1992) The methanogenic bacteria. In: Barlows A, Truper HG, Dworkin M, Harder W, Schleifer KH (eds.) The prokaryotes. 2nd edition, Springer-Verlag, New York

Wolf-Gladrow DA, Zeebe RE, Klaas C, Körtzinger A, Dickson AG (2007) Total alkalinity: The explicit conservative expression and its application to biogeochemical processes. Mar Chem 106: 287–300. https://doi.org/10.1016/j.marchem.2007.01.006

Yamamoto S, Alcauskas J B, Crozier TE (1976) Solubility of methane in distilled water and seawater. J Chem Eng Data 21: 78–80. https://doi.org/10.1021/je60068a029

Yu Z, Wang D, Li Y, Deng H, Hu B, Ye M, Zhou X, Da L, Chen Z, Xu S (2017) Carbon dioxide and methane dynamics in a human-dominated lowland coastal river network (Shanghai, China). J Geophys Res Biogeosciences 122 : 1738–1758. https://doi.org/10.1002/2017JG003798

Xu Y-Y, Pierrot D, Cai W-J (2017) CO2 SYS Ocean carbonate system computation for anoxic waters using an updated CO2SYS program. Mar Chem 195:90-93. https://doi.org/10.1016/j.marchem.2017.07.002

Zhai W, Dai M, Guo X (2007) Carbonate system and CO_2 degassing fluxes in the inner estuary of Changjiang (Yangtze) River, China. Mar Chem 107:342–356. https://doi.org/10.1016/j.marchem.2007.02.011

Table 1 Mean, standard deviation, minimum, and maximum values of the main water properties of JLC investigated in this study, separated in "river" and "lagoon" stations, for all sampling campaigns.

	Temp. (°C)	Salinity	pH (NBS)	Chl *a* (µg L^{-1})	DO (%sat)	TA (µmol kg^{-1})	DIC (µmol kg^{-1})	pCO_2 (ppmv)	CH_4 (nmol L^{-1})	$N\text{-}NH_4^+$ (µmol L^{-1})
Mar-2017										
Rivers	26.6 ± 1.1 23.9 / 27.7	1.0 ± 1.1 0.2 / 4.0	7.09 ± 0.07 7.02 / 7.26	7.1 ± 12.9 0.2 / 30.2	2.1 ± 1.7 0.1 / 6.1	3,004 ± 194 2,618 / 3,313	3435 ± 306 3012 / 3846	13,641 ± 3,211 8,931 / 16,974	47,285 ± 22,731 25,573 / 70,913	2,154 ± 990 887 / 3,333
Lagoons	27.5 ± 1.1 25.9 / 29.0	19.3 ± 3.6 11.2 / 24.9	7.90 ± 0.05 7.84 / 7.97	13.9 ± 9.9 5.3 / 30.4	57.4 ± 23.9 24.3 / 86.2	1,868 ± 338 1,431 / 2,263	1802 ± 401 1,385 / 2,233	872 ± 240 577 / 1,226	392 ± 304 92 / 723	312 ± 249 129 / 677
Jun-2017										
Rivers	22.5 ± 0.3 22.2 / 23.4	0.2 ± 0.0 0.2 / 0.3	7.12 ± 0.08 6.93 / 7.22	0.6 ± 0.2 0.3 / 0.9	3.9 ± 0.8 (2.0 5.5	1,400 ± 836 572 / 3,268	1,663 ± 1,408 652 / 4,028	6,878 ± 7,801 1,927 / 20,417	43,637 ± 17,408 30,677 / 68,336	2,542 ± 432 1,028 / 3,477
Lagoons	22.9 ± 1.0 22.0 / 24.6	16.1 ± 5.2 6.6 / 24.8	8.10 ± 0.43 7.63 / 8.67	17.0 ± 7.1 9.58 / 26.71	81.8 ± 38.9 35.0 / 140.0	1,694 ± 229 1,497 / 2,047	1,599 ± 358 1,267 / 2,032	821 ± 708 109 / 1,603	1,415 ± 1,878 47 / 4,660	104 ± 45 58 / 177
Nov-2017										
Rivers	25.6 ± 0.6 24.9 / 26.7	1.2 ± 1.5 0.2 / 5.1	7.51 ± 0.45 7.13 / 8.64	73.3 ± 153.5 2.1 / 347.9	28.2 ± 42.7 1.0 / 135.0	2,949 ± 466 2,450 / 3,680	3,029 ± 755 2,003 / 3,918	8,127 ± 5,066 218 / 13,742	159,178 ± 105,131 550 / 288,572	3,353 ± 1,721 868 / 5,660
Lagoons	21.6 ± 1.3 20.4 / 24.2	26.9 4.9 21.2 / 31.8	8.12 ± 0.09 8.04 / 8.30	34.6 ± 35.4 3.6 / 77.0	87.4 ± 12.2 73.1 / 112.0	2,169 ± 495 1,449 / 2,567	1,975 ± 515 1,205 / 2,287	523 ± 217 215 / 725	1,121 ± 1,610 199 / 3,528	35 ± 47 3.5 / 105
May-2018										
Rivers	25.9 ± 0.4 25.3 / 26.6	0.6 ± 0.4 0.2 / 1.6	7.18 ± 0.22 6.97 / 7.63	-	1.7 ± 0.4 1.4 / 2.8	2,860 ± 265 2,399 / 3,062	3,226 ± 259 2,853 / 3,560	11,500 ± 5,398 3,856 / 17,096	-	3,126 ± 1,348 768 / 4,078
Lagoons	24.9 ± 1.0 23.7 / 27.2	26.0 ± 5.6 16.0 / 34.0	7.92 ± 0.04 7.84 / 7.97	24.0 ± 5.9 18.3 / 32.7	71.0 ± 9.4 52.4 / 85.6	2,173 ± 326 1,659 / 2,441	2,055 ± 292 1,594 / 2,319	843 ± 117 716 / 981	-	294 ± 332 96 / 876

Table 2 Average values of gas exchange velocity (k_{600}), and air-water CO_2 and CH_4 fluxes calculated according to Wanninkhof (1992), Raymond and Cole (2001) (RC01) and Jiang et al. (2008) (J08), separated by river and lagoon stations, and integrated for entire superficial area, for each sampling campaign.

	k_{600} cm h^{-1}			CO_2 flux mmol m^{-2} d^{-1}			CH_4 flux mmol m^{-2} d^{-1}		
	W92	RC01	J08	W92	RC01	J08	W92	RC01	J08
Mar-2017									
Rivers (1.07 Km^2)	2.84	4.88	5.10	363.34	624.33	652.48	38.19	65.63	68.59
Lagoons (12.08 Km^2)	2.24	4.40	4.75	8.95	17.59	18.99	0.24	0.48	0.51
All system area-weighted (13.15 Km^2)				37.78	66.95	70.50	3.33	5.78	6.05
Jun-2017									
Rivers (1.07 Km^2)	2.06	4.24	4.64	126.25	259.86	284.38	22.58	46.47	50.85
Lagoons (12.08 Km^2)	1.12	3.44	4.15	4.46	13.70	16.53	0.38	1.18	1.42
All system area-weighted (13.15 Km^2)				14.36	33.72	38.32	2.19	4.86	5.45
Nov-2017									
Rivers (1.07 Km^2)	0.99	3.32	4.09	72.85	244.32	300.98	44.80	150.27	185.12
Lagoons (12.08 Km^2)	4.50	6.24	6.13	4.27	5.93	5.82	1.12	1.56	1.53
All system area-weighted (13.15 Km^2)				9.85	25.32	29.83	4.68	13.66	16.47
May-2018									
Rivers (1.07 Km^2)	2.24	4.24	4.75	237.85	450.21	504.37			
Lagoons (12.08 Km^2)	2.06	4.40	4.64	7.25	15.49	16.33			
All system area-weighted (13.15 Km^2)				26.01	50.86	56.04			

Table 3 Stoichiometry of main diagenetic reactions that significantly affect TA in the environment. The reactions were separated in positive TA alterations (most common in anaerobic environments), and negative TA alterations (most common in aerobic environments). * Exceptions are the reactions of precipitation and dissolution of $CaCO_3$, which are not necessarily linked to aerobic/anaerobic conditions.

			Net Change	
	Positive TA alterations	Chemical Reaction	DIC	TA
1	Ammonification	$R\text{-}NH_2H + H_2O + H^+ \rightarrow R\text{-}OH + NH_4^+$	0	+2
2	Denitrification	$CH_2O + 0.8NO_3^- + 0.8H^+ \rightarrow CO_2 + 0.4N_2 + 1.4H_2O$	+1	+0.8
3	Iron reduction	$CH_2O + 2Fe_2O_3 + 8H^+ \rightarrow CO_2 + 5H_2O + 4Fe^{2+}$	+1	+8
4	Sulphate reduction	$2CH_2O + SO_4^{2-} + 2H^+ \rightarrow 2CO_2 + 2H_2O + H_2S$	+2	+2
5	Manganese reduction	$CH_2O + 2MnO_2 + 3H^+ \rightarrow HCO_3^- + 2Mn^{2+} + 2H_2O$	+1	+4
6	$CaCO_3$ dissolution *	$CaCO_3 \rightarrow 2CO_3^{2-} + 2Ca^{2+}$	+1	+2
			Net Change	
	Negative TA alterations	Chemical Reaction	DIC	TA
7	Nitrification	$NH_4^+ + 2O_2 \rightarrow NO_3^- + 2H^+ + H_2O$	0	-2
8	Iron oxidation	$Fe^{2+} + O_2 + 10H_2O \rightarrow 4Fe(OH)_3 + 8H^+$	0	-8
9	Sulfide oxidation	$1/2HS^- + O_2 \rightarrow 1/2SO_4^{2-} + 1/2H^+$	0	-1
10	Manganese oxidation	$2Mn^{2+} + O_2 + 4HCO_3^- \rightarrow 2MnO_2 + 4CO_2 + 2H_2O$	0	-4
11	$CaCO_3$ precipitation *	$2Ca^{2+} + 2CO_3^{2-} \rightarrow CaCO_3$	-1	-2

Table 4 Average values of CO_2 equivalent emissions (CO_2eq) calculated for CO_2 and CH_4 degassing. The fluxes were calculated for "rivers" and "lagoons" stations, and after integrated for the entire superficial area, for each sampling campaign. The fluxes were calculated using the gas transfer velocity of Raymond and Cole (2001) (RC01).

	CO_2 emissions in CO_2eq g CO_2-eq m^{-2} d^{-1}	CH_4 emissions in CO_2eq * g CO_2-eq m^{-2} d^{-1}	Weight of CO_2 (%) (in CO_2eq)	Weight of CH_4 (%) (in CO_2eq)
Mar-2017				
Rivers(1.07 km^2)	27.47	29.40	48.30	51.70
Lagoons (12.08 km^2)	0.77	0.21	78.23	21.77
All system area-weighted (13.15 km^2)	2.94	2.58	53.21	46.79
Jun-2017				
Rivers	11.43	20.81	35.45	64.55
Lagoons	0.72	0.69	51.01	49.99
All system area-weighted	1.48	2.17	40.51	59.49
Nov-2017				
Rivers	10.73	67.20	13.77	86.23
Lagoons	0.26	0.62	29.42	70.58
All system area-weighted	1.11	6.11	15.40	84.60

* Fluxes of CH_4 multiplied by 28, which represents the GWP of CH_4 (IPCC, 2013).

Fig. 1

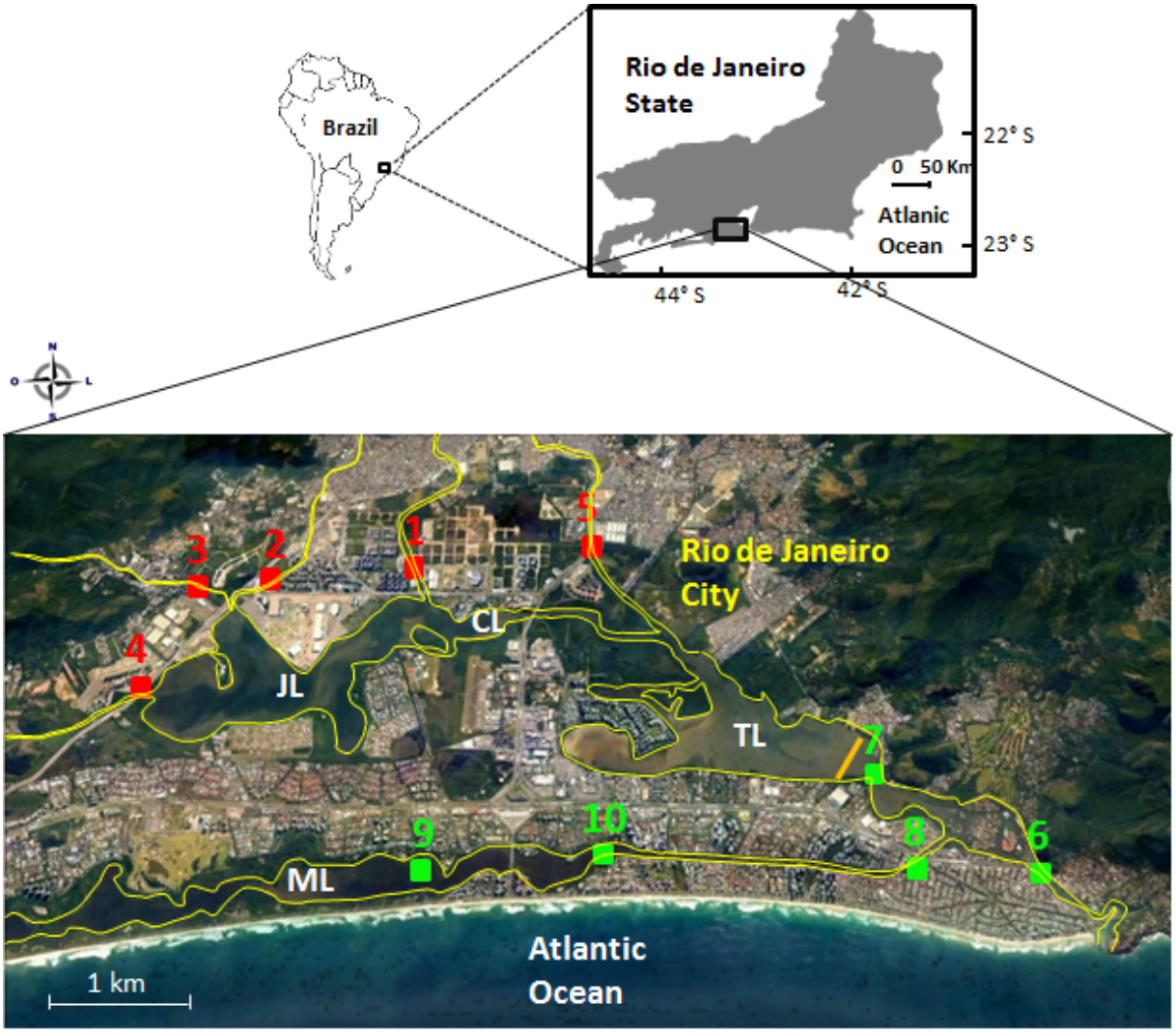
Brazil
Rio de Janeiro State
0 50 Km
Atlanic Ocean
22° S
23° S
44° S
42° S
N
O
L
S
1
2
3
4
5
6
7
8
9
10
CL
JL
TL
ML
Rio de Janeiro City
Atlantic Ocean
1 km

Fig. 2

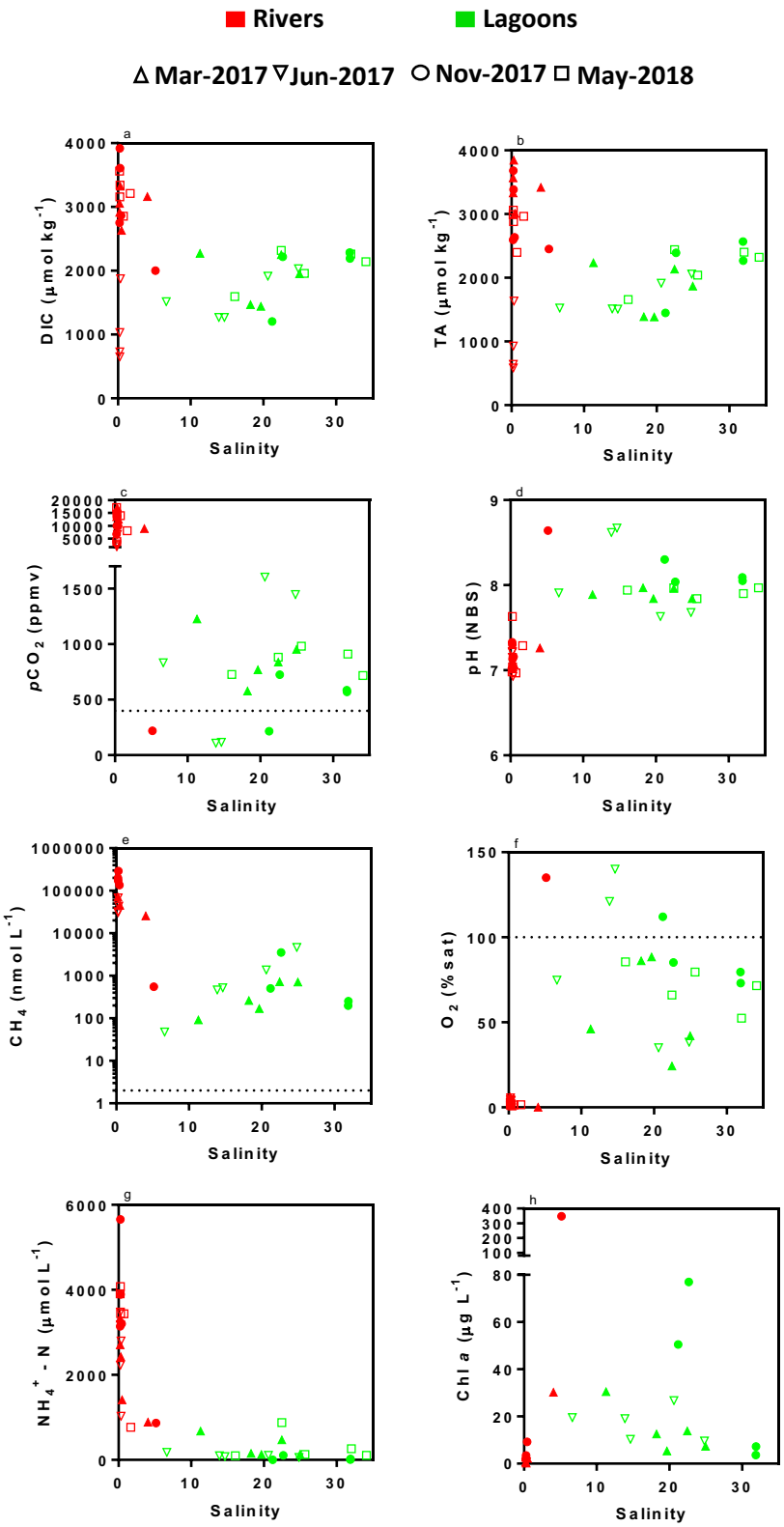
Rivers
Lagoons
Mar-2017
Jun-2017
Nov-2017
May-2018
a
DIC (µmol kg-1)
b
TA (µmol kg-1)
c
pCO2 (ppmv)
d
pH (NBS)
e
CH4 (nmol L-1)
f
O2 (% sat)
g
NH4+ - N (µmol L-1)
h
Chl a (µg L-1)
Salinity

Fig. 3

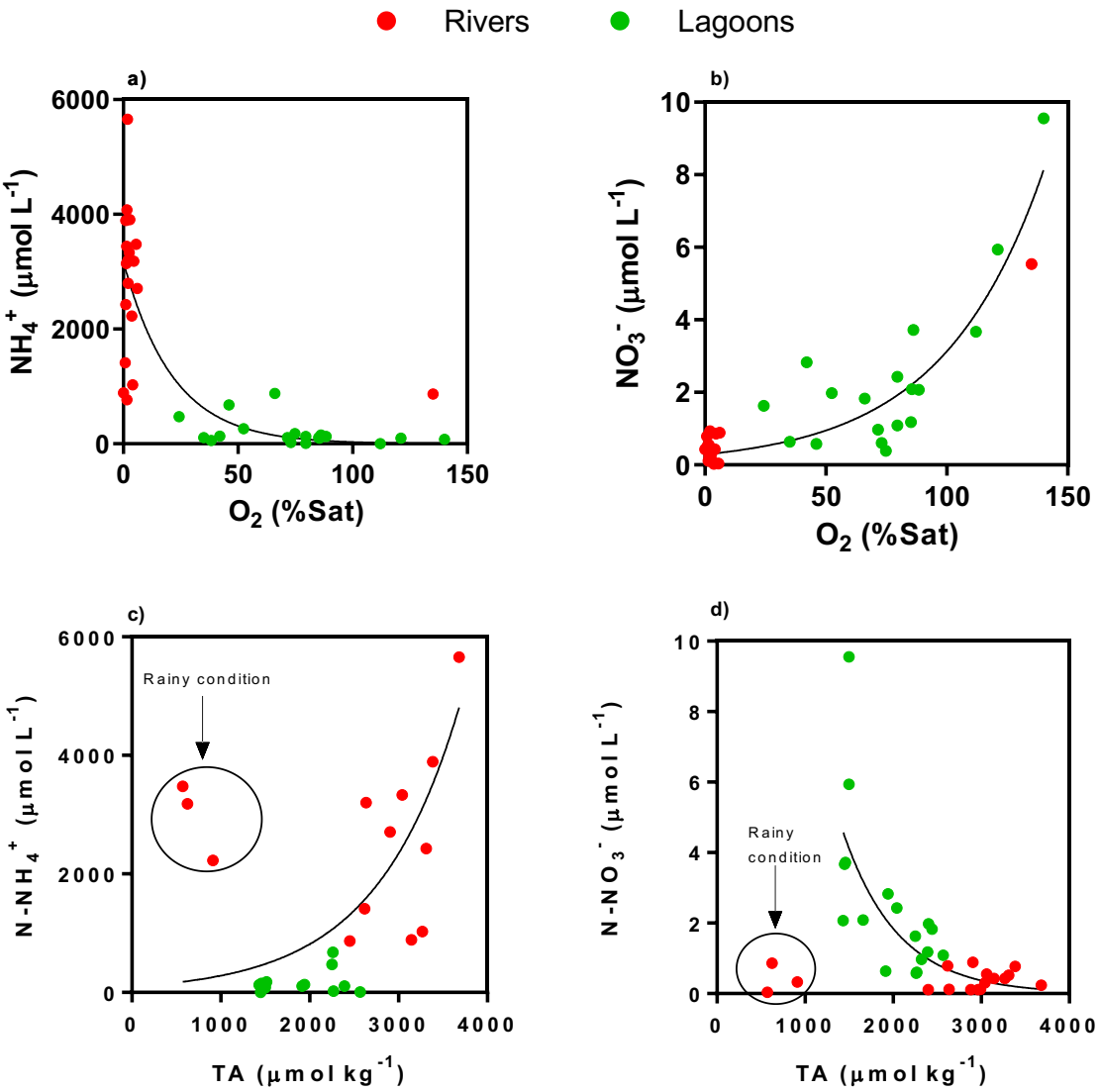
Rivers
Lagoons
a)
NH_4^+ (µmol L^{-1})
O_2 (%Sat)
b)
NO_3^- (µmol L^{-1})
O_2 (%Sat)
c)
N-NH_4^+ (µmol L^{-1})
Rainy condition
TA (µmol kg^{-1})
d)
N-NO_3^- (µmol L^{-1})
Rainy condition
TA (µmol kg^{-1})

Fig. 4

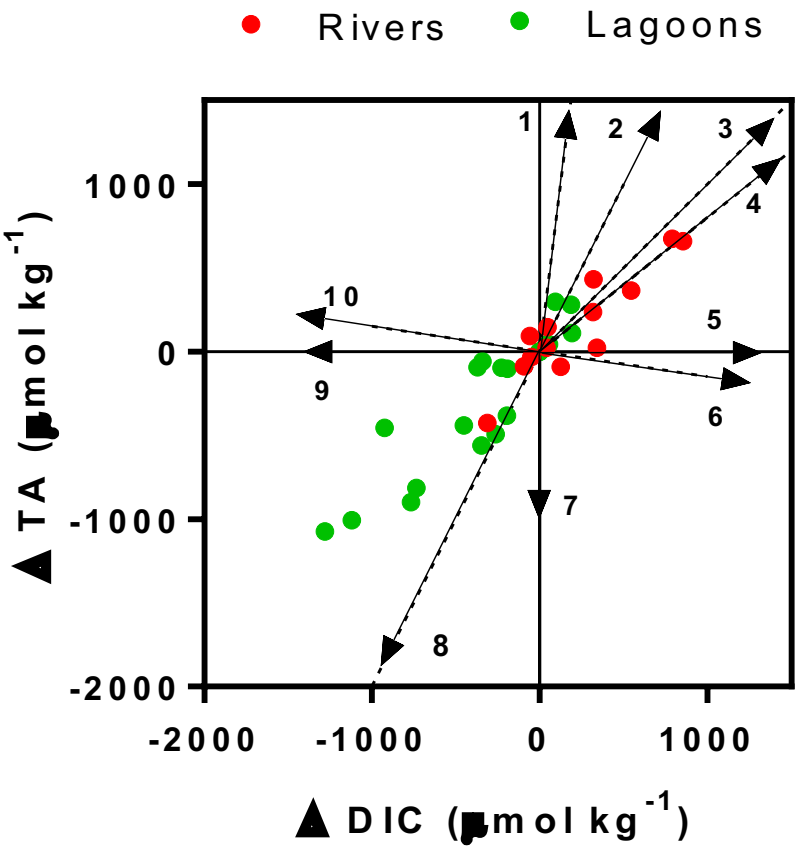
Rivers
Lagoons
1
2
3
4
5
6
7
8
9
10
1000
0
-1000
-2000
-2000
-1000
0
1000
▲TA (μmol kg-1)
▲DIC (μmol kg-1)

Fig. 5

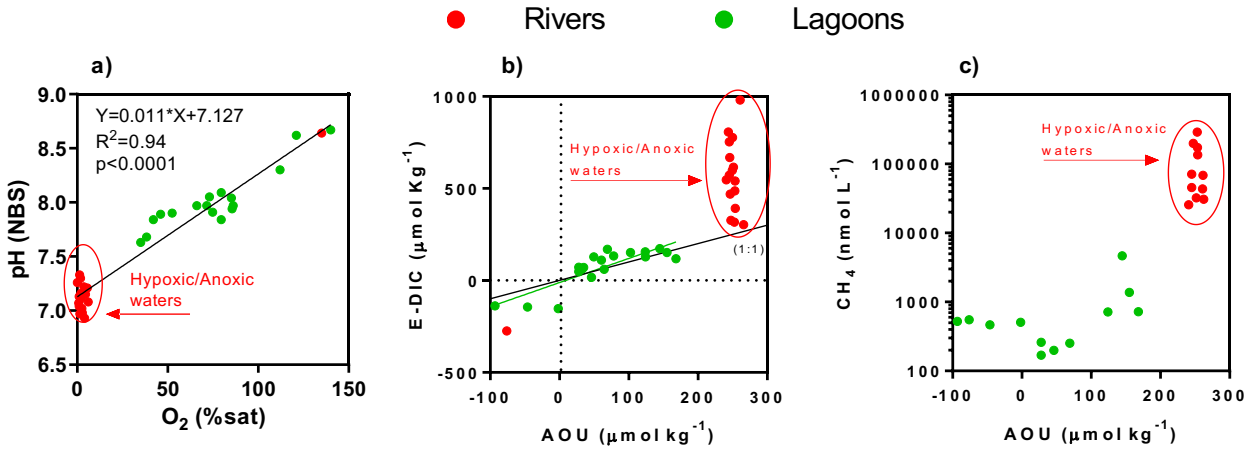
Rivers
Lagoons
a)
Y=0.011*X+7.127
R2=0.94
p<0.0001
Hypoxic/Anoxic waters
pH (NBS)
O2 (%sat)
b)
Hypoxic/Anoxic waters
(1:1)
E-DIC (µmol Kg-1)
AOU (µmol kg-1)
c)
Hypoxic/Anoxic waters
CH4 (nmol L-1)
AOU (µmol kg-1)

Fig. 6

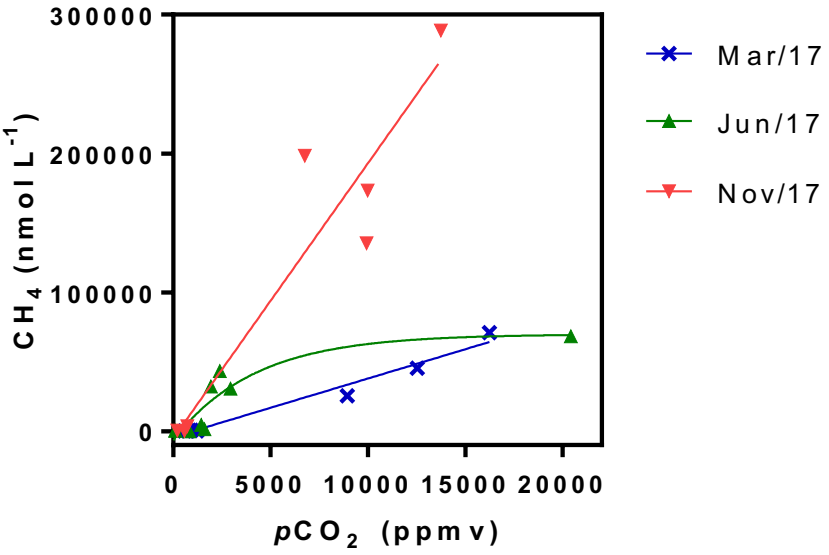

Electronic Supplementary Material

Greenhouse gas emissions (CO_2 and CH_4) and inorganic carbon in an urban tropical coastal lagoon (Jacarepagua Lagoon Complex, Brazil)

Luiz C. Cotovicz Jr.*[a,b]; Renato P. Ribeiro[c]; Carolina Ramos Régis[b]; Marcelo Bernardes[b]; Rodrigo Sobrinho[b]; Luciana Oliveira Vidal[d]; Daniel Tremmel[b]; Bastiaan A. Knoppers[b]; Gwenaël Abril[b,e]

Affiliations

a Instituto de Ciências do Mar, Universidade Federal do Ceara, Fortaleza, CE, Brazil

b Programa de Geoquímica, Universidade Federal Fluminense, Niterói, RJ, Brazil

c Instituto Federal de Educação, Ciência e Tecnologia do Rio de Janeiro (IFRJ), Nilópolis, RJ, Brasil

d Laboratório de Ciências Ambientais, Centro de Biociências e Biotecnologia Universidade Estadual do Norte Fluminense, Campos dos Goytacazes, RJ, Brazil

e Biologie des Organismes et Ecosystèmes Aquatiques (BOREA), UMR 7208, Muséum National d'Histoire Naturelle, CNRS, IRD, SU, UCN, UA, Paris, France.

* Corresponding Author: lccjunior@id.uff.br; Telephone Number (+55 21 995645663); ORCID 0000-0002-3914-8155

Fig. S1 Box plots (maximum, percentile 75%, median, percentile 25% and minimum) of the main parameters analyzed in this study for all sampling campaigns, separated by sampling stations (1-10). The horizontal lines in plots b), d), e) represent the atmospheric values.

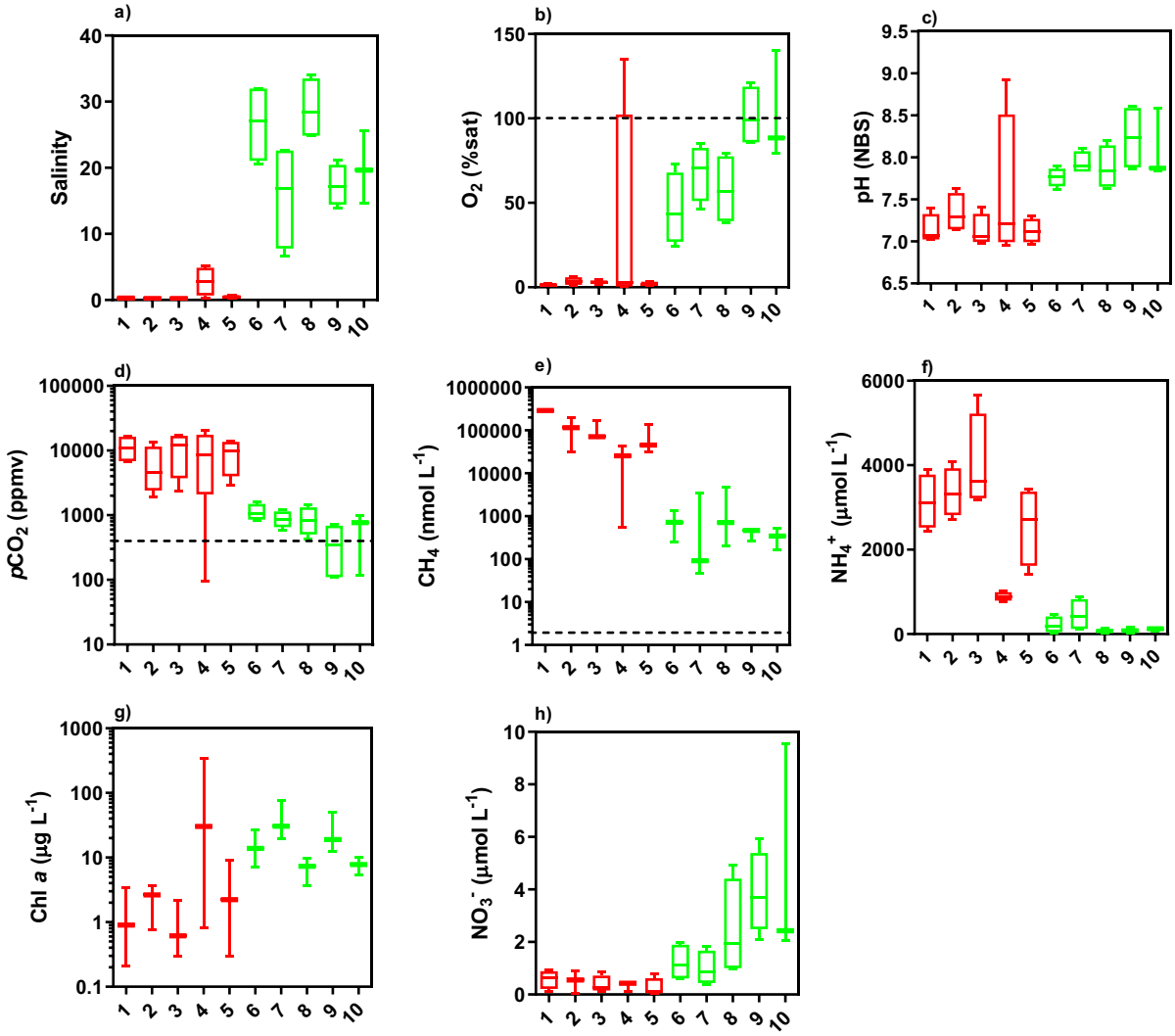

Fig. S2 Emissions of CO_2 and CH_4 calculated averaging the fluxes including the three parameterizations of gas transfer velocity, which were Wanninkhof (1992), Raymond and Cole (2001), Jiang et al. (2008). The fluxes were calculated considering river and lagoon stations separately, and integrated for entire superficial area, comprising all sampling campaigns. Note that graphs are in logarithm scales.

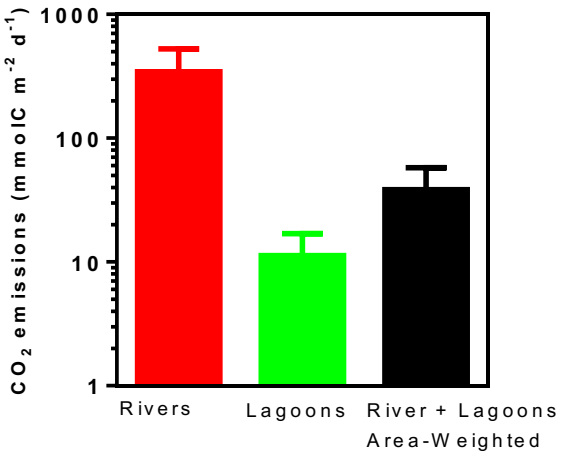
CO_2 emissions (mmolC m^{-2} d^{-1})
1000
100
10
1
Rivers
Lagoons
River + Lagoons
Area-Weighted

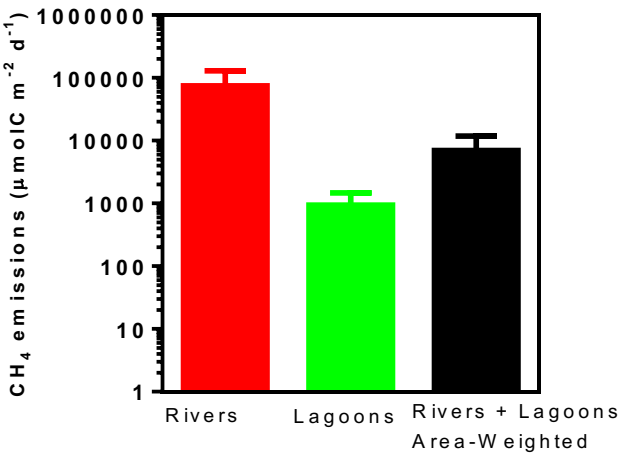
CH_4 emissions (µmolC m^{-2} d^{-1})
1000000
100000
10000
1000
100
10
1
Rivers
Lagoons
Rivers + Lagoons
Area-Weighted